IODOPERFLUOROHEXANE AS A LASANT FOR IODINE LASERS

A Thesis

Presented to

the Graduate College

In Partial Fulfillment

of the Requirements for the Degree of

Master of Science

by

Clarence L. Wells

July 1990

This thesis submitted by Clarence L. Wells in partial fulfillment of requirements for the Degree of Master of Science in Physics at Hampton University, Hampton, Virginia, is hereby approved by the committee under whom the work has been done.

Bagher M. Tabibi
Dr. Bagher M. Tabibi

Dr. Demetrius D. Venable

Dr. Ja H. Lee

Dr. Demetrius D. Venable
Dean of the Graduate College

7-30-90
Date

REPORT DOCUMENTATION PAGE

Form Approved
OMB No. 0704-0188

1. AGENCY USE ONLY (Leave Blank)	2. REPORT DATE	3. REPORT TYPE AND DATES COVERED
	Aug 1990	Final

4. TITLE AND SUBTITLE
Iodoperfluorohexane as a Lasant for Iodine Lasers

5. FUNDING NUMBERS

6. AUTHOR(S)
Captain Clarence L. Wells

7. PERFORMING ORGANIZATION NAME(S) AND ADDRESS(ES)
Hampton University
Department of Physics
Hampton, VA 23665

8. PERFORMING ORGANIZATION REPORT NUMBER

9. SPONSORING/MONITORING AGENCY NAME(S) AND ADDRESS(ES)

10. SPONSORING/MONITORING AGENCY REPORT NUMBER

11. SUPPLEMENTARY NOTES

12a. DISTRIBUTION/AVAILABILITY STATEMENT

12b. DISTRIBUTION CODE

13. ABSTRACT (Maximum 200 words)

See abstract copy with each thesis.

14. SUBJECT TERMS

15. NUMBER OF PAGES
74

16. PRICE CODE

17. SECURITY CLASSIFICATION OF REPORT	18. SECURITY CLASSIFICATION OF THIS PAGE	19. SECURITY CLASSIFICATION OF ABSTRACT	20. LIMITATION OF ABSTRACT
(UNCLASSIFIED)			

ABSTRACT

Iodoperfluorohexane as a Lasant for Iodine Lasers

Student: Captain Clarence L. Wells Department: Physics

[redacted] Advisor: Dr. Bagher M. Tabibi

A comparative analysis is made of iodoperfluorohexane, $C_6F_{13}I$ to iodoperfluoropropane, C_3F_7I when used as the gain medium in an iodine laser system. Parameters for this comparison are the absorption cross section in the pumpband 250 to 290 nanometers, laser output energy, and the production of molecular iodine (I_2), the major quenching by-product of iodine laser reactions. This study confirms that $C_6F_{13}I$ has an absorption cross section that is almost equal to C_3F_7I and laser output energy as high as 1.5 times greater. The amount of I_2 produced is less in $C_6F_{13}I$ due to an I_2 elimination and recombination processes that are yet to be fully understood. Theses. (55)

ACKNOWLEDGEMENT

I would like to express my appreciation to Dr. Bagher M. Tabibi and to Dr. Demetrius D. Venable for the patience and support provided during this graduate period. Additional, gratitude goes to Dr. Ja. H, Lee who impressed upon me both the desire to work more diligently, as well as the relationships between research, discipline, and success. Individual thanks goes to Dr. James C. Davenport my undergraduate professor. Special thanks goes to my family and to my fiancee who supplied constant support in the belief that I would succeed. This research was supported in part by the NASA Langley Research Center's Advanced Solar Energetics Program under grant number NASA NAG-1-400. Personal support was provided by the U.S. Army under the fully funded civil school program in accordance with Army Regulation 621-1.

TABLE OF CONTENTS

LIST OF TABLES

LIST OF FIGURES

LIST OF PLATES

Chapter 1

Introduction

In 1964 work by Kasper and Pimentel resulted in the first iodine photodissociation laser[8]. Lasing occurred due to photolysis in the $^2P_{1/2}$ to $^2P_{3/2}$ transition of atomic iodine. Used in this first test were CF_3I and CH_3I. The laser emission, at 1.315 μm, was the result of pumping in the absorption band 250 to 290 nanometers. Continued testing of these and other photodissociative lasing compounds have revealed numerous differences. These differences can be the determining factor in the use of a specific chemical as the gain media for a laser system.

A. Background

Interest in laser pumping by solar radiation began at NASA about 1977. A solar pumped laser provided direct energy conversion without electric power from photovoltaic cells[1]. This goal has pursued three distinct sources. Pumping of a photodissociation type laser, a molecular gas laser with devices of an absolute blackbody arrangement or of a solid state laser. The advantages and disadvantages of each (Table 1) will be debated until deployment of the first orbital system. At NASA Langley Research Center, a photodissociation iodine laser has been studied. This system was initially proven feasible by Lee and Weaver[2] in 1981. Light from a xenon arc that simulated solar radiation at air mass zero (AM0) or in

TABLE 1.

Comparison of Solar Pumped Lasers

Type of Laser	Active Medium	Threshold solar Concentration for gain = 2-5 x 10^4 cm^{-1} X (1.35W/m^2)	Limiting Efficiency* (η_{lim}, %)
Photodissociation	RI*	~10^2	2-3
	IBr	~2 * 10^3	5
	CO_2 - Br_2	20 - 30	6
Gasdynamic closed-cycle	CO_2	~10^3	6
Pumped by IR radiation of absolute blackbody	CO_2	~10^3	1
Solid-state waveguide	Nd^{3+} w/ impurity ions 160		4

*Limiting efficiency is defined by the efficiencies of the system:

$h_{lim} = h_{sp} \times h_q$ for Photodissociation system,

$= h_{sp}$ (blackbody) x h_{sp} (CO_2) x h_q for Blackbody system and

$= h_{sp} \times h_q \times h_l$ for Solid State system;

where h_q =quantum efficiency, h_{sp} =spectral efficiency, and h_l = quantum efficiency of luminescence.

(Reference 4)

---

outer space was chopped and focused into a conical reflector for lasing pumping.

The NASA research program seeks to discover the laser system's ideal parameters. One major factor is the lasant. Space applications requires lasants with the qualities:

(1) Gas or liquid,

(2) High temperature operation,

(3) Chemical reversibility, and

(4) Broadband pumping.

Various alkyl iodides such as n-C_3F_7I, i-C_3F_7I, C_2F_5I, n-C_4F_9I and t-C_4F_9I that meet this criterion have been found and tested. Testing of iodoperfluorohexane ($C_6F_{13}I$) was to confirm whether this chemical had advantages over those already considered. This study is significant for it can result in a more efficient space laser system. Presently, t-C_4F_9I is considered the best chemical for this purpose due to its high output and near 100 percent reversibility[3]. Perfluorohexane has shown some properties that give it advantages over the C_3F_7I. Earlier test of perfluoro alkyl iodides for iodine lasers indicated improved properties with heavier molecules[4].

A xenon flashlamp was used to simulate solar radiation during this research. The system (Plate 1) was composed of a 0.152-m flashlamp coupled to a quartz laser tube that was 6 mm ID and 0.254-m long. The pumping length was 0.152 m. The mirror cavity length was 0.460 m with a

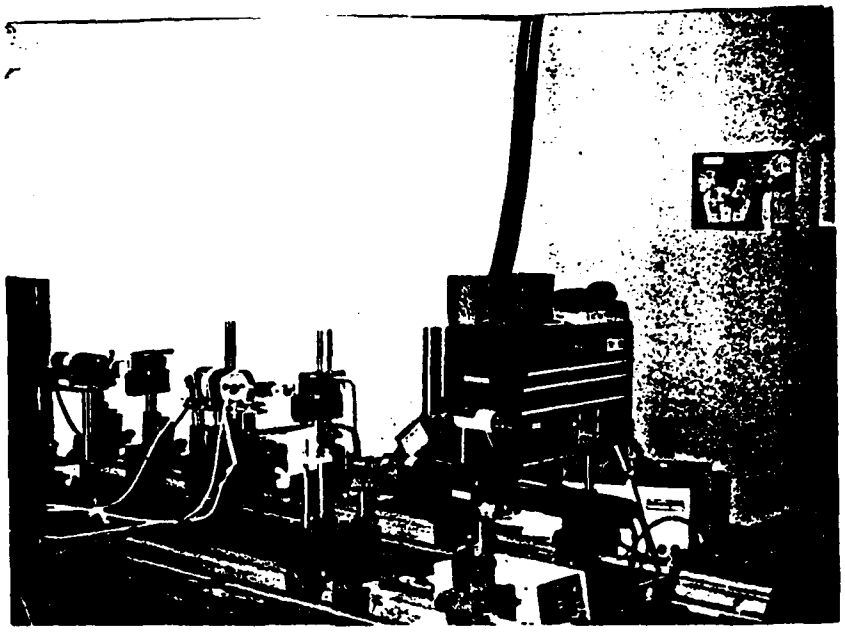

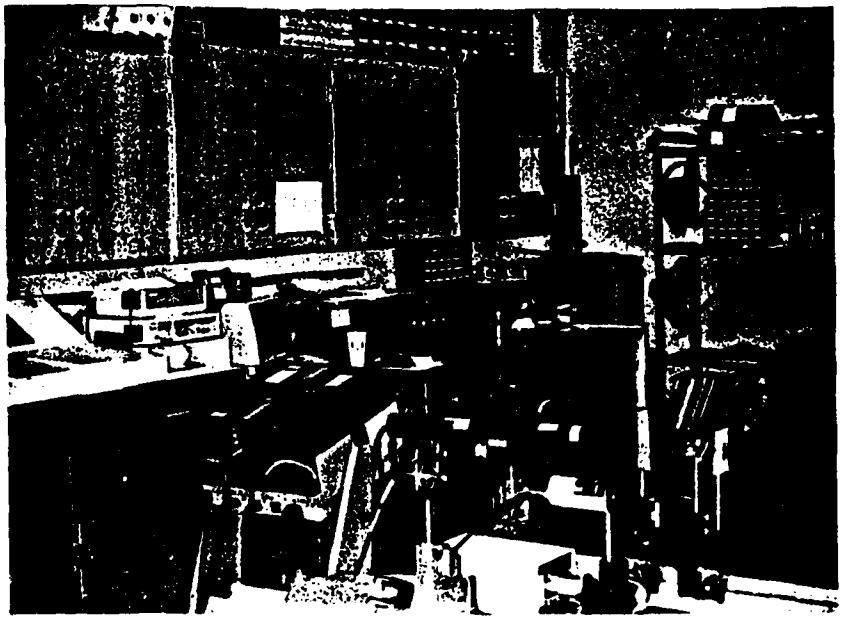

Plate 1 The iodine laser system. The top frame shows the system mounted upon an optical table with the vent system for toxins and monitoring devices. Digital data acquisition equipment is shown in the lower frame.

96 percent output mirror and a maximum reflectivity rear mirror. A silicone photodiode (EG&G model SGD-040) was used to monitor the flashlamp emission.

The laser output was monitored by a germanium detector (Molectron model J-16). Direct energy measurements were made by a pyroelectric energy meter (Molectron model J-3). The lasant was stored in a glass flask at room temperature. Filling of the laser tube was by evaporation. Used chemical was collected by condensation in a collection flask submersed in liquid nitrogen.

This thesis research compares the laser performance of perfluorohexyl iodide (n-$C_6F_{13}I$) to that of perfluoropropyl iodide (n-C_3F_7I). The latter chemical has undergone extensive testing in the past, therefore ample information is available to use it as the baseline for the comparison. Compared parameters are the maximum output energy, the dependence of each chemical on pump energy and gas pressure and the laser performance when a single gas charge is repeatedly pumped. These parameters were measured for laser operations with both fresh and used chemicals.

B. The Laser Process

The following discussion on the laser process is based on reference 26. In any laser system, light amplification occurs through stimulated emission of photon energy from atoms that have been excited (pumping) into an upper level (designated by subscript 2). The probability that an

excited atom will undergo spontaneous emission by transition to the lower level (designated by subscript 1) in a time interval dt is

$$A_{21}\,dt = \frac{1}{\tau_{21}}dt \tag{1.1}$$

where A_{21} is the spontaneous transition rate and τ_{21} is the lifetime of the atom in an excited state.

Emission from an excited level also may occur through photon stimulation. For a system in equilibrium, the upward and downward transitions may be defined by:

$$N_1\rho B_{12} = N_2\,\rho B_{21} + N_2\,A_{21}$$

yielding the energy density

$$\rho = N_2\,A_{21} / N_1 B_{12} - N_2 B_{21}\,. \tag{1.2}$$

The terms A_{21}, B_{12} and B_{21} are called Einstein coefficients where B_{12} and B_{21} are stimulated transition rates upward and downward respectively and N represents population density. Applying Boltzman statistics for a system in thermal equilibrium to (1.2) give the ratio

$$N_1/N_2 = g_1/g_2\,\exp\,[(E_2-E_1)/kT] = g_1/g_2\,\exp(h\nu\,/kT)$$

or

$$\rho = A_{21}/B_{21}\;/\;[g_1\,B_{21}/\,g_2\,B_{12}\,\exp(h\nu\,/kT)] - 1; \tag{1.3}$$

where g_1 and g_2 are the degeneracies of each level, ν is the frequency of the absorption photon, h is Planck's constant, k is Boltzman's constant and T is

the temperature of the system in Kelvin degrees.

This system is similar to a blackbody, where

$$\rho = 8\pi h\nu^3 / c^3 \, [1/\exp(h\nu /kT) - 1]; \qquad (1.4)$$

and c is the speed of light. Comparing (1.3) and (1.4) provides

$$g_1B_{12}=g_2B_{21} \quad \text{and} \quad A_{21}/B_{21} = 8\pi h\nu^3/c^3$$

The ratio of spontaneous emission to stimulated emission can then be expressed as

$$R = A_{21}/\rho B_{21} = \exp(h\nu /kT) - 1. \qquad (1.5)$$

which indicates R > 1 for a system at equilibrium. Therefore, lasing requires a non-equilibrium distribution of atoms. Specifically, the population density N_2 of the upper level must increase above the population density N_1 of the lower level. Accomplishment of this condition is called population inversion. Figure 1 indicates systems at thermal equilibrium and at population inversion. The mechanism used to obtain population inversion in this work is optical pumping. Pumping requires input of energy into the system at a high rate, which produces an intermediate level in which the rate of spontaneous transition back to the lowest level is small compared to the rate of decay to the upper laser level. Inspection of the ratio $A_{21}/\rho B_{21}$ in (1.5) clearly shows the requirement of input energy to change this equilibrium condition to R > 1.

The iodine laser is optically pumped for population inversion.

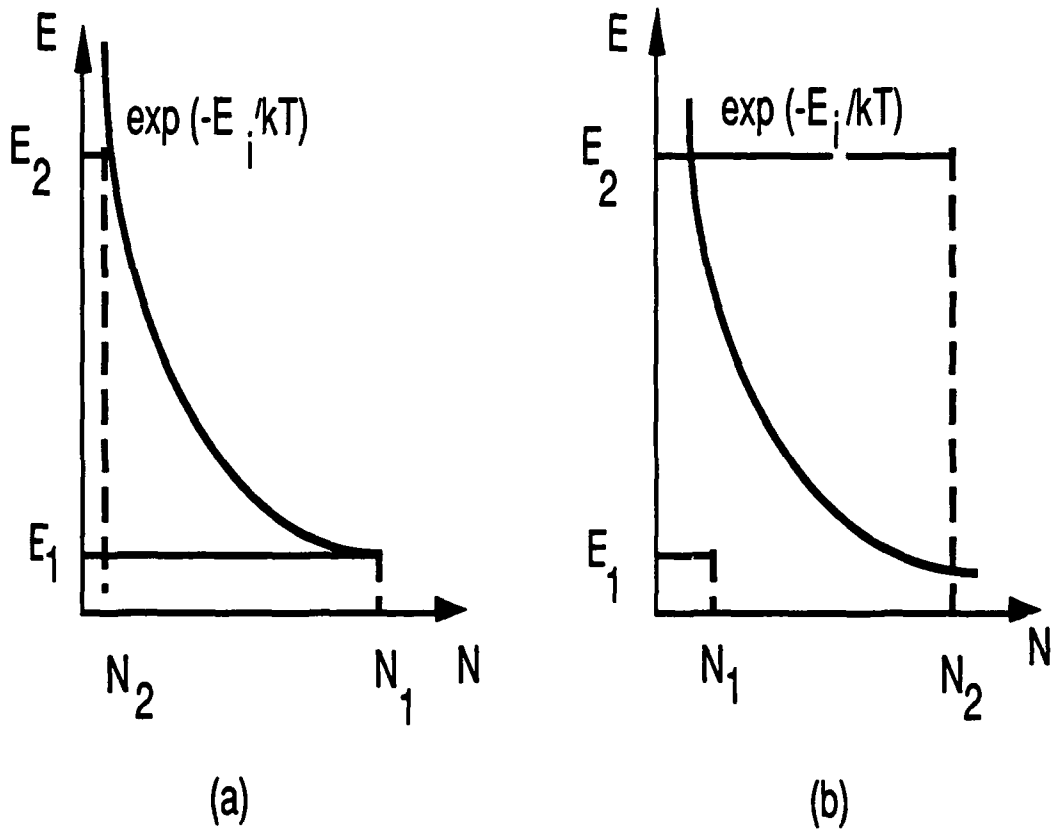

Figure 1. The population density of 2 systems. System (a) is at thermal equilibrium and (b) after population inversion. Energy levels (E_1 and E_2) are specified vertically and the corresponding number densities (N_1 and N_2) horizontally.

Energy input into this system is absorbed by the laser medium, i.e. iodides ($C_nF_{2n+1}I$). Determination of the absorption uses Lambert Law [5]

$$dI/dx = -\alpha I(x)$$

or

$$I = I_o \exp(-\alpha x)$$

where

I_o - the incident irradiance,

α - absorption coefficient, and

x - length of the sample penetrated.

Absorption will depend on the atoms N_1 in the lowest level and N_2 in the upper level.

Consider a volume element of thickness Δx and unit cross-sectional area. From (1.2) and (1.5) using the stimulated absorption (B_{12}) and stimulated emission (B_{21}) the net rate loss of photons per unit volume is defined as :

$$-dN/dt = (g_2/g_1\, N_1 - N_2)\, \rho_1 B_{21} - N_2 A_{21}.$$

If no contribution to the laser will be made by N_2A_{21}, then this expression reduces to

$$-dN/dt = (g_2/g_1\, N_1 - N_2)\, \rho\, B_{21}. \qquad (1.6)$$

Recall that $I=\rho c/n$ where n is the index of refraction and c is the velocity of

light. Then $I(\nu) = \rho_\nu c/n = N h\nu\, c/n$. Therefore, the change in photon density by passing through the volume elements is

$$-dN(x) = [I(x) - I(x + \Delta x)]\, n/h\nu_{21}c.$$

If $\Delta x \rightarrow 0$, then

$$-dN(x) = [-dI(x)/dx][n/h\nu_{21}c].$$

In the time interval $dt = \Delta x /(c/n)$

$$dN/dt = dI(x)/dx\ (1/h\nu_{21}).$$

From Lambert's Law $dI/dx = -\alpha I(x)$

and

$$dN/dt = -\alpha I(x)/h\nu_{21} = -\alpha\rho_\nu c/n(1/h\nu_{21}).$$

The absorption coefficient α is then equal to

$$\alpha = (g_2/g_1\ N_1 - N_2) B_{21} h\nu_{21} n.$$

The ratio g_2/g_1 is normally on the order of 1, yielding

$$\alpha = (N_1 - N_2) B_{21}\ h\nu_{21}\ n. \qquad (1.7)$$

The positive α confirms the original conditions for a system in thermal equilibrium. However, the laser condition requires $N_2 > N_1$ and therefore α is negative. Lambert's Law can then define the amplification of the stimulating beam as it passes through the medium with

$$I = I_o \exp(Kx) \qquad (1.8)$$

where K is the small signal gain coefficient

$$K = (N_2 - g_2/g_1 N_1) B_{21} h\nu_{21} n/c.$$

To begin lasing there exists a minimum number of atoms required in the excited level. This value is considered the threshold of the system. The gain coefficient, must also have a minimum value to maintain laser oscillation. This value may be reduced by:[5]

1. Transmission at the mirrors,
2. Absorption and scattering at the mirrors,
3. Absorptions in the laser medium which do not contribute to lasing,
4. Scattering at optical inhomogeneities in the laser medium (minute affect in iodine laser systems), and
5. Diffraction losses at the mirror.

Grouping these losses into one loss coefficient γ and introducing it into (1.8) yields

$$I = I_o \exp[(K - \gamma) L]$$

where L replaces x as the laser cavity length. The round trip gain is

$$G = r_1 r_2 \exp [2 (K - \gamma) L]$$

where r_1, r_2 are the reflectances of the rear and output mirrors. The gain must be greater than or equal to 1 for the oscillation to grow. Therefore, the minimum gain is 1, and the threshold condition is

$$G = r_1 r_2 \exp [2(K_{th} - \gamma)L] = 1 \qquad (1.9)$$

with

$$K_{th} = \gamma + 1/2L \ln(1/ r_1 r_2)$$

where K_{th} is the threshold gain coefficient.

Expressions (1.8) and (1.9) assume that 100 percent of the atoms in the upper level interact with the stimulating photon beam. The probability of this occurring is restricted due to the spectral width of this photon. A Gaussian curve can be used to represent the probability of a given transition from level E_2 to E_1. This curve, called the lineshape function $g(\nu)$, identifies the emission (or absorption) of a photon with frequency between ν and $\nu + d\nu$. Normalization of $g(\nu)$

$$\int_{-\infty}^{\infty} g(\nu)\, d\nu = 1,$$

places the peak wavelength of this spectral width at the middle of the distribution. The Füchtbauer-Landerburg relation relates the area under this absorption curve to the Einstein coefficients and the populations of each energy level. The interaction of the stimulated emission beam (monochromatic) of frequency ν_s with the atoms of the upper level with a lineshape $g(\nu)$ yield the small signal gain

$$K(\nu_s) = (N_2 - g_2/g_1\, N_1)B_{21}\, h\nu_s\, n\, g(\nu_s)/c. \qquad (1.10)$$

The shape of the lineshape function is affected by Doppler broadening, collisional (or pressure) broadening and natural (or lifetime)

damping. These mechanisms are classified as either homogeneous or inhomogeneous broadening. Inhomogeneous broadening mechanisms yield the Gaussian frequency distribution

$$g(\nu)_G = 2/\Delta\nu\ (\ln 2/\pi)^{1/2} \exp[-(\ln 2)\ (\nu - \nu_o)/\ \Delta\nu/2)^2]$$

where $\Delta\nu$ the linewidth ν_o is the peak frequency.

For $\nu = \nu_o$

$$g(\nu_o)_G = 2/\Delta\nu\ (\ln 2/\pi)^{1/2}.$$

A good approximation of this value is

$$g(\nu_0) \approx 1/\Delta\nu \tag{1.11}$$

with $\Delta\nu$ approximated[6] as

$$\Delta\nu = (2/\lambda)\ (2RT \ln 2 / M)^{1/2}. \tag{1.12}$$

where R is the universal gas constant and T is absolute temperature, and M is molecular weight.

Evidence of these mechanisms are shown in the hyperfine structure. The laser transition $5^2P_{3/2}$ shows hyperfine divisions into six lines. Figure 2 indicates the hyperfine splitting of this transition. The hyperfine spectra is due to the magnetic moment of the iodine nucleus. This effect was not studied in detail in this research for the effect was systematic and was therfore present for both chemicals.

The threshold inversion density dN_{th} is now defined. Combining equations (1.9) and (1.10) results in the expression

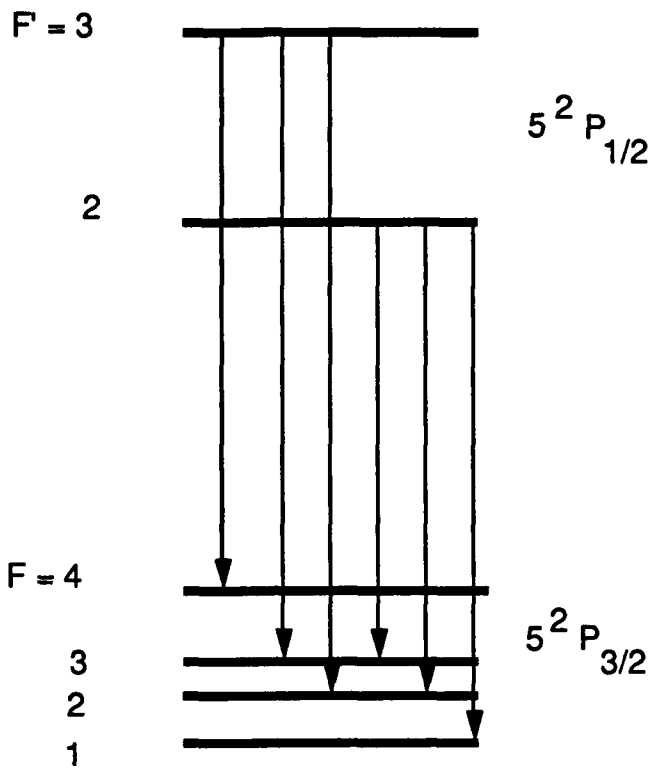

Figure 2. The hyperfine structure for atomic iodine. Six transitions are found between the $5^2P_{1/2}$ --- $5^2P_{3/2}$ levels. Radiative transition are shown by the arrows.

$$(N_2 - g_2/g_1\, N_1)_{th} = K_{th} c / B_{21} h\nu_s n g(\nu_s).$$

The stimulated emission transition rate B_{21} was defined as

$$B_{21} = c^3 A_{21} / (8\pi h\nu^3 n^3).$$

Substitution for B_{21} and $g(\nu_s)$ gives

$$\Delta N_{th} = 8\pi\nu_o^2 K_{th} \tau_{21} \Delta\nu\, n^2 / c^2 \qquad (1.13)$$

where τ_{21} has replaced A_{21} to represent the lifetime of the upper excited level. The system used in this study had a threshold inversion density (based on reflectivities 0.99 and 0.96 and cavity length 0.125 m) of

$$\Delta N_{th} = 7.70 \times 10^{14} / cm^3.$$

There also exists a minimum pump power necessary to produce the threshold inversion density. The iodine laser is a four level system (ie. E_0-ground state, E_3-excited state, E_2-meta-stable state, E_1-intermediate state), which reduces the required pump power for population inversion. Figure 3 shows a four level system. A determination of the minimum pump power began with an analysis of these levels. Assume that $E_1 >> KT$ and that the population density ΔN_{th} is small.

Specify R_2 and R_1 as the pumping rates into levels 2 and 1 respectively. Therefore, the rate equations for those levels are

$$dN_2/dt = R_2 - N_2 A_{21} - \rho_\nu B_{21} (N_2 - N_1) \qquad (1.14)$$

and

$$dN_1/dt = R_1 + \rho B_{21}(N_2 - N_1) + N_2A_{21} - N_1A_{10} \quad (1.15)$$

Assuming steady pumping provides

$$dN_2/dt = dN_1/dt = 0$$

Using this fact to solve (1.14) and (1.15) yields

$$N_1 = R_2/A_{10}$$

$$N_2 = R_2 [1 + \rho_\nu B_{21}/ A_{10}] (A_{21} + \rho_\nu B_{21})^{-1}$$

combine

$$N_2 - N_1 = R_2 [(1- A_{21}/A_{10})/A_{21} + \rho_\nu B_{21}] \quad (1.16)$$

Figure 3 shows that $A_{21} < A_{10}$ must hold to produce a positive numerator. A negative numerator means $N_2 < N_1$ and population inversion has not occurred. The Einstein coefficients A_{21} and A_{10} are defined by

$$A_{1N} = 1/\tau$$

where τ is the spontaneous lifetime of the level and N is a positive integer. The required population inversion will occur if $\tau_{10} < \tau_{21}$ or $A_{21} < A_{10}$. For $\tau_{21} >> \tau_{10}$ the normal lasing condition, $(1 - A_{21}/A_{10}) \approx 1$ holds. Just before threshold ρ_ν may be neglected, reducing (1.16) to

$$N_2 - N_1 = R_2 [(1 - A_{21}/A_{10})/ A_{21}]. \quad (1.17)$$

Imposing the afore mentioned condition provides the threshold relation

$$N_{th} = R_{th} A_{21}$$

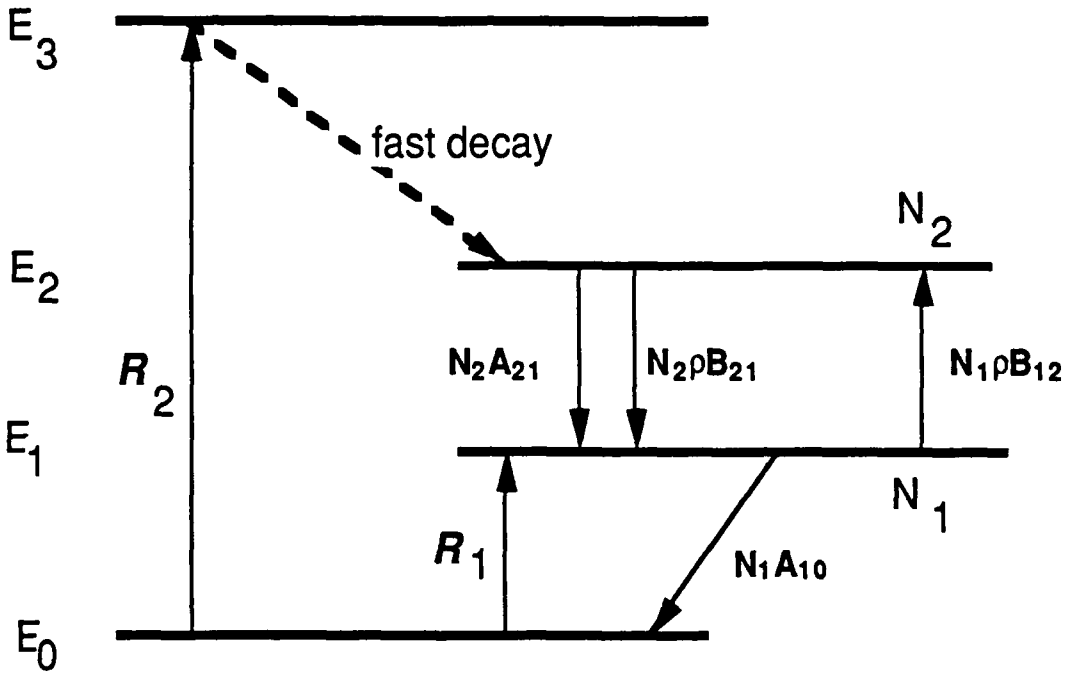

Figure 3. A four level laser system. E_o represents the ground level, E_1 the terminal level, E_2 the metastable level and E_3 the excited level. The pumping rate is indicated as R_2.

or

$$Rth = N_{th}/\tau_{21}. \tag{1.18}$$

Each atom reaching the excited level acquire an amount of energy E_3. The total pump power per unit volume at threshold is then

$$P_{th} = E_3 N_{th}/ \tau_{21}.$$

or substitution of (1.13)

$$P_{th} = E_3 8\pi \nu_o^2 K_{th} \Delta\nu n^2. \tag{1.19}$$

An equilibrium now exist where gain equals cavity losses. Now combining (1.17) and (1.18) gives

$$R_{th}/A_{21} = R_2 / A_{21} + \rho_\nu B_{21}$$

yielding

$$\rho_\nu = A_{21}/B_{21} (R_2/R_{th} - 1). \tag{1.20}$$

Output power W is directly proportional to the optical power density within the laser cavity. The pump rate into the excited level is proportional to the pump power P delivered to the laser. Accordingly, (1.20) can be written as

$$W = W_o (P/P_{th} - 1).$$

Figure 4 shows the linearity of pumping rate and laser output. This confirms the balance of gain and losses at and beyond threshold values.

Other expressions exist for threshold inversion density.[7] The density can be related directly to the small signal gain through combining expressions (1.9) and (1.13) yielding

$$G = \exp(2\sigma_s \Delta N_{t\,h} L) \qquad (1.21)$$

where, L is the cavity length and σ is the stimulated emission cross section4 equal to 6.5 x 10-18 cm2 .

It is also approximated by

$$N_2 \approx t_f W / h\nu V \qquad (1.22)$$

where N_2 is the number of atoms in the upper level

t_f is the time of pumping,

$h\nu$ is the photon energy at the absorption wavelength,

V is the volume of the laser tube, and

W is the power of the pump.

Because $N_1 << N_2$, once population inversion occurs, the value $\Delta N_{th} = (N_2 - N_1)$ is approximated to equal N_2.

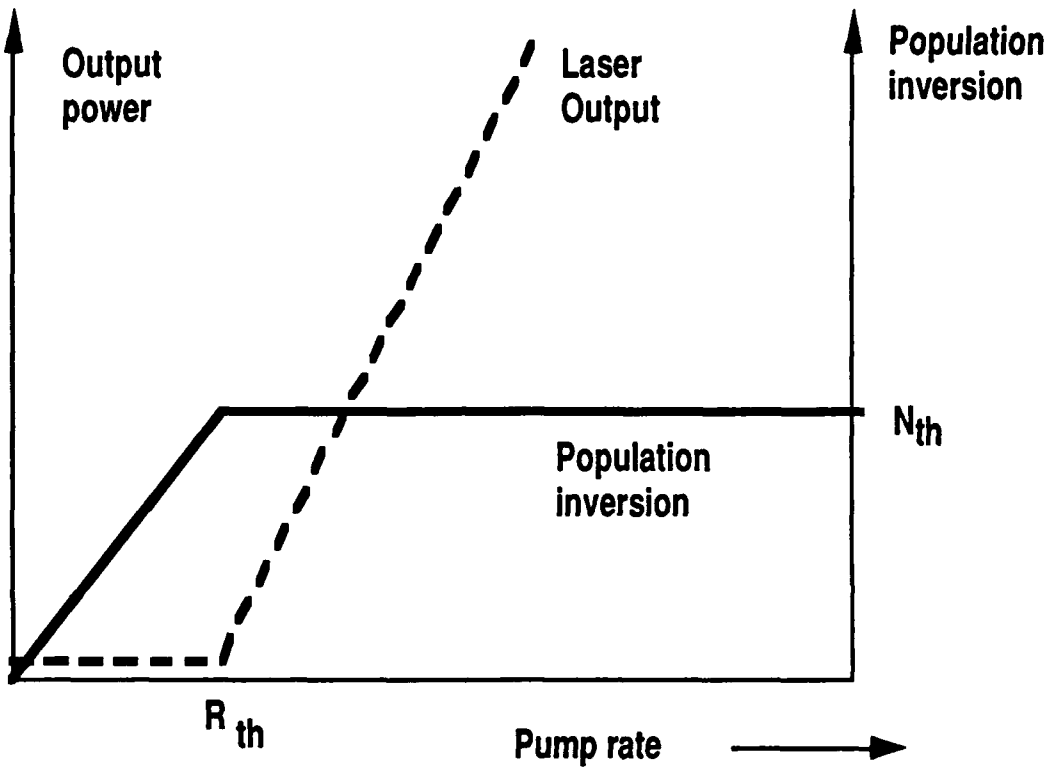

Figure 4. Population inverison and laser output as a function of the pump rate. Beyond threshold pumping the laser output continues to increase while the population inversion remains constant.

Chapter 2

Iodine Laser Processes

Although simple in design, the iodine laser is influenced by numerous factors. These factors include, the chemical properties, photolysis, quantum yield, favorable (unfavorable) reactions, absorption cross-section and quenching agents.

A. Perfluoroalkyl Iodides

Several iodine compounds exist which are highly reactive or photosensitive. The selection of alkyl iodides for use in a laser system stem from the early study of the absorption spectra of these compounds. In 1938 Porrett and Goodeve[8] found that photolysis produced excited iodine. This was the foundation of Kasper and Pimentel research, which produced the first iodine laser. At this time both hydrated alkyl and perfluoroalkyl iodides were used. It was found that perfluoroalkyl iodides were superior[6] over hydrated alkyl iodides due to the quantum yield of excited iodine atoms. In addition, the rate constants (see kinetic reactions) for collisional deactivation were significantly higher for hydrated alkyl iodides, leading to lower laser output. More recent research points to the possibility that heavier fluorinated alkyl iodides[2] are better candidates for iodine lasers. The heavier molecular weight and increased specific heat would produce

more excited iodine while a greater heat capacity means higher temperature operation than less complex molecules. Table 2 show the physical properties of the iodides used in this study.

B. Photodissociation and Reactions

As stated in Chapter 1, the iodine laser operates by photodissociation of iodine atoms from the parent molecules ($C_nF_{2n+1}I$) to produce atomic iodine. Iodine bonding to the parent molecule leaves an unbonded electron. Initial excitation of this electron changes it to an antibonding (p*) orbit, which results in the antibonding potential[9]

$$Vn(r) = E^* + Do + A \exp[-a(r - r_e)] \qquad (2.1)$$

where E^* is the $I(^2P_{1/2})$ excitation energy, D_o is the C-I bond energy, r is the C-I bond length and A, a, and r_e are related to the absorption and the wavelength of the absorption peak for the chemical. Figure 5 shows the change from an attractive to a repulsive potential for R-I and R-I* bonding. The photon energy causes photodissociation of molecule according to the reaction

$$RI + h\nu \rightarrow R + I^* \qquad (2.2)$$

where R represents the radical C_nF_{2n+1}. Excited iodine is continually pumped into the $5^2P_{1/2}$ level until population inversion is produced. At this time the population of the lower $5^2P_{3/2}$ level is just one-half of the upper level and the inversion density is

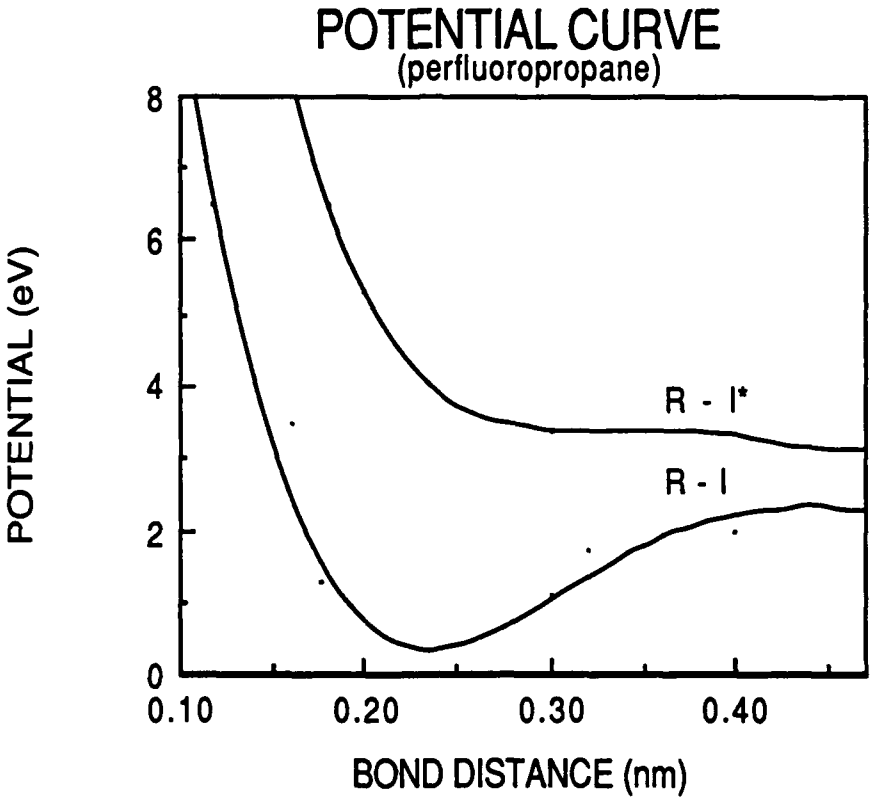

Figure 5. The potential curves of C_3F_7I for the R -I and R -I* bonds. As energy absorption occurs (excited level) the R - I bond changes to a replusive potential.

TABLE 2.

Physical Properties of Measured Iodides

	C_3F_7I	$C_6F_{13}I$
Molecular Weight	295.2 amu	445.95 amu
Density	2.06 g/cm^3 @ 20^{0}C	2.06 g/cm^3 @ 25^{0}C
Boiling Point	40 ^{0}C / 760 mm Hg	58 ^{0}C / 80 mm Hg
Vapor Pressure	350 Torr @ 760 mm Hg	16 Torr @ 760 mm Hg
Index of Refraction	1.3272 @ sodium D line	1.3275 @ sodium D line

---

$$\Delta N=[I^*] - 1/2[I] \qquad (2.3)$$

where [I*] is the population density of the iodine atoms in the $5^2P_{1/2}$ level (Excited State) and [I] is the population density of the iodine atoms in the $5^2P_{3/2}$ level (Ground State).

Equation (1.9) indicated the round trip gain as

$$G= r_1r_2\exp(2\sigma \Delta NL).$$

The gain is defined as the ratio of the output signal of the system for a small input signal at the emission frequency. The inversion density can then be related to gain at threshold by

$$\Delta N = -.5\ln(r_1 r_2)/\sigma L \qquad (2.4)$$

where G= 1 at threshold. Other reactions influence the build-up of excited iodine in the metastable level before reaching threshold. Among these are the following:

$$R + I^* \xrightarrow{K_1} RI \qquad (2.5)$$

where, R is the radical C_nF_{2n+1}

I* is excited iodine in the $5^2P_{1/2}$ level,

RI is the parent molecule C_nF_{2n+1} I, and

K_1 is the kinetic rate coefficient of the reaction.

$$R + I \xrightarrow{K_2} RI \qquad (2.6)$$

where I is iodine in the $5^2P_{3/2}$level and

K_2 is the kinetic rate coefficient of the reaction.

$$R + R \xrightarrow{K_3} R_2 \qquad (2.7)$$

where R_2 is a dimmer (di-molecule), formed by the

combination of two radicals, and

K_3 is the kinetic rate coefficient of the reaction.

$$R + RI \xrightarrow{K_4} R_2 + I \qquad (2.8)$$

where K_4 is the kinetic rate coefficient of the reaction.

Quenching reactions reduce or eliminate the number of I* atoms in the metastable level. These reactions include:

$$RI + I^* \xrightarrow{Q_1} RI + I, \tag{2.9}$$

$$I^* + I_2 \xrightarrow{Q_2} I + I_2, \tag{2.10}$$

and

$$I^* + O_2 \xrightarrow{Q_3} I + O_2.$$

where O_2 is the pressure of oxygen due to vacuum system leaks or diffused gas in components of the laser system.

Three body reactions are

$$I^* + I + RI \xrightarrow{C_1} I_2 + RI, \tag{2.11}$$

$$I + I + RI \xrightarrow{C_2} I_2 + RI, \tag{2.12}$$

$$I^* + I + I_2 \xrightarrow{C_3} I_2 + I_2, \tag{2.13}$$

and

$$I + I + I_2 \xrightarrow{C_4} I_2 + I_2. \qquad (2.14)$$

A complete list of these reactions with the corresponding rate coefficients for C_3F_7I is found in Table 3. No references were found, which contained reactions and rate coefficients for $C_6F_{13}I$. The speeds at which these reactions occur determines the full effect on the laser. Reactions bearing rate coefficients which are very slow have little impact on the inversion density. Other reactions play a significant role. These equations combine to form the kinetic processes of the iodine laser system.

C. Kinetic Processes

Figure 6 illustrates the major kinetic of the iodine laser. Shown are the pumping, fast decay, stimulated emission and some of the chemical processes. From this diagram it is clearly seen which reactions increase laser output and which reduce (or quench) lasing. Two reactions produce the same product, but their individual affect on the laser is diametrically different. The reactions

$$\text{(a) } R + I^* \rightarrow RI \quad \text{and} \quad \text{(b) } R + I \rightarrow RI$$

are each important for a closed laser system. These are the principle reactions by which the lasant is recovered. They differ in that (a) depopulates the $5^2P_{1/2}$ level reducing the probability of reaching population

TABLE 3.

Iodine Laser Reactions and Rate Coefficients for C_3F_7I

REACTANTS	PRODUCT	SYMBOL	RATE COEFFICIENT [$(cm^3)^n/sec$]
R + R	R_2	K_3	2.6×10^{-12}
R + I	RI	K_2	2.3×10^{-11}
I + I + RI	I_2	C_2	8.5×10^{-32}
I + I + I_2	$I_2 + I_2$	C_4	3.8×10^{-30}
R + RI	R_2 + I	K_4	3.0×10^{-16}
R + I*	RI	K_1	5.6×10^{-13}
I* + RI	I + RI	Q_1	2.0×10^{-16}
I* + I_2	I + I_2	Q_2	1.9×10^{-11}
I* + I + RI	I_2 + RI	C_1	3.2×10^{-33}
I* + I + I_2	$I_2 + I_2$	C_3	8.0×10^{-32}
R + RI	R_2 + I*	K_5	3.2×10^{-17}
I* + RI	RI_2*	K_6	8.3×10^{-18}

n is an integer used to designate the complexity of the molecule.

(Reference NASA Technical Paper 2241)

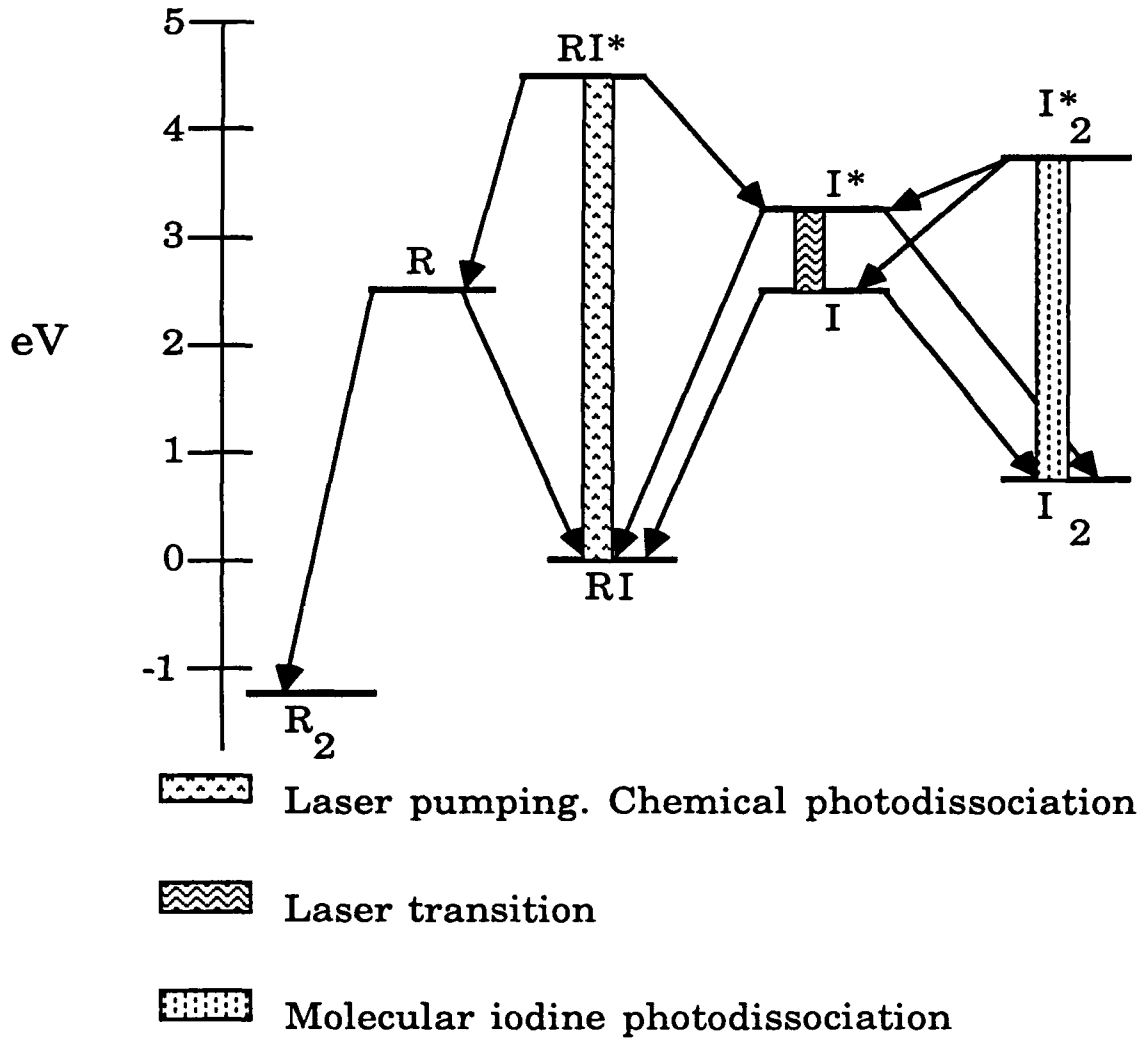

Figure 6. The primary kinetics of iodine laser systems. Three transitions are shown. Optical pumping of the parent molecule RI by ultraviolet radiation absorption, excited iodine I* transition to a lower level as the result of stimulated emission, and optical pumping of molecular iodine I_2 by visible radiation absorption.

inversion. The opposite exist for (b) for this reaction reduces the population of the terminal level $5^2P_{3/2}$ thereby assisting the achievement of population inversion.

By far the greatest impact on lasing is caused by molecular iodine. As shown by equations (2.10 to 2.14), molecular iodine or I_2 is the strongest quenching agent of the laser. Although I_2 is photosensitive, it does not strongly photodissociate when excited by light in the visible range (400-700nm) to produce an appreciable quantity of atomic iodine. Perfluoroalkyl iodides with large quantities of this impurity have a tell-tail pink or reddish color. Obtaining laser output from a lasant contaminated in this way requires high pumping rates. Studies have found[10] that photodissociation of alkyl iodides in the absence of a laser field results in the combination of I* into molecular iodine. In this case, the efficiency of the reaction $R + I^* \rightarrow RI$ is reduced, such that recombination back to the parent molecule is slowed.

The kinetic rate coefficient (indicated by a letter and subscript), of each reaction equation, specifies the time rate of change in the densities of the reactants and product. In a reaction with reactants C and D yielding the product A the rate coefficient is

$$R_1 = \frac{d[A]/dt}{[D][C]} \quad \text{for } C + D \xrightarrow{R_1} A. \tag{2.15}$$

Assuming one atom or molecule of each reaction forms one product atom or molecule, then

$$d[C]/dt = -d[A]/dt. \tag{2.16}$$

With this foundation the rate coefficients for (2.9), (2.11) and (2.14) are defined in terms of I* rate of change as

$$K_1 = -d[I^*]/dt/[R]\,[I^*], \tag{2.17}$$

$$Q_1 = -d[I^*]/dt/[RI]\,[I^*], \tag{2.18}$$

$$C_1 = -d[I^*]/dt/[I^*]\,[I]\,[RI, \tag{2.19}$$

and

$$C_4 = -d[I^*]/dt/[I^*]\,[I]\,[I_2]. \tag{2.20}$$

Comparing these equations to the actual rates from Table 3, shows the dependence of I* population on the speed of the reaction.

D. Diffusional Mixing

When photolyzed in a cylindrical tube a number of the original molecules N_a per unit volume are irreversibily[11] decomposed. After photolysis, diffussional mixing cause the concentrations of decomposed and parent chemical to equilibrate. This diffusional mixing will be controlled by the one dimensional diffusional equation giving the concentration N_i of species i in the tube as a function of time and position in

$$\frac{\partial N_1}{\partial t} = D_i \frac{\partial^2 N_i}{\partial x^2} \tag{2.21}$$

where D_i is the diffusion coefficient of species i in the surrounding mixture. With boundary conditions of specie i at time zero, $N_i\ (x,0) \equiv \phi_i\ (x)$

immediately following photolysis. Expression (2.21) then has solution[11]

$$N_i(x,t) = .5(\pi D_i t)^{-1/2} \int_{-\infty}^{\infty} \phi_i(u) \exp[-(x-u)^2 / 4D_i du$$

where x is the distance from the center of the photolysis region and u - is an undefined absorption variable.

The shot to shot decomposition is relatively small, so the parent molecule remains the dominant species. Therefore continued lasing and more importantly chemical reversibility remain possible.

E. Absorption of Light

Pumping of the iodine laser system is by the intense light of a xenon flashlamp. Both pulses as short as 2.7 ms (FWHM) or as long as 140 ms (FWHM) are used in pumping. The pump duration, T_p is limited by [6]

$$T_p \leq d / 4a_s \{\Delta E / E - \varphi l / d\} \qquad (2.22)$$

where d is the diameter of the laser tube,

a_s is the velocity of the light shockwave,

l is the pumping length of the laser tube,

φ is the beam divergence, and

$\Delta E/E$ is the fractional energy loss.

Light is coupled into the laser tube by the geometry of the reflector. Figure 7 shows the laser tube and flashlamp mounted parallel within a cylinder. The cylinder effectively forms two parabolic reflectors, with the laser tube

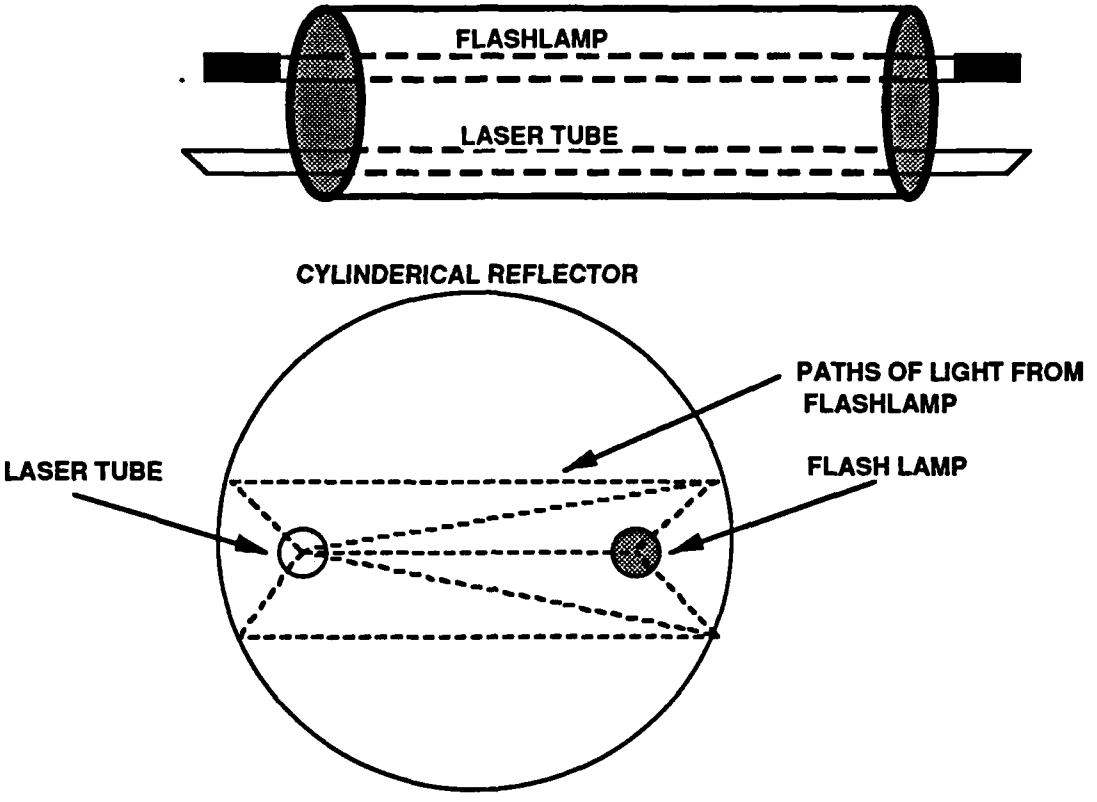

Figure 7. Light coupling from a xenon flashlamp into the quartz laser tube. The reflector is cylindrical with aluminum used as the reflective surface.

mounted at the foci of each reflector. Light from the flashlamp is focused along the optical center of the laser tube. The light undergoes small attenuation passing through the two interfaces of the laser tube. The quartz laser tube has ultraviolet transmission between 90-92 percent. This attenuation is also a function of the radial angle at which the light enters the laser tube. Light reaching the laser tube at angles approaching 90 and 270 degrees, relative to the plane of the laser tube and flashlamp have lower intensity than that at 0 or 180 degrees.

The xenon flashlamp intensity in the ultraviolet (UV) region peaked near 300nm, which corresponds to a blackbody temperature of 9600 kelvin. From Planck's Radiation Law,[5]

$$I_\lambda = 2\pi hc^2 / \lambda^5 [1 / \exp(hc / \lambda kT) - 1] \qquad (2.23)$$

The photon flux for a blackbody is given by

$$\phi_\lambda d\lambda = 2\pi c / \lambda^4 [\, d\lambda / \exp(hc / \lambda kT) - 1] \qquad (2.24)$$

where c is the speed of light,

h is Planck's constant, and

$\phi_l \, d\lambda$ is the photon flux on the wavelength interval

between λ and $\lambda + d\lambda$.

The iodine absorption band is 250 to 290 nm. Measured in this range the spectral irradiance of the light coupling into the laser tube is

$$I_p(\lambda) = \int_{250}^{290} I(\lambda)\, d\lambda$$

or

$$I_p(\lambda) = \int_{250}^{290} I_0(\lambda l)[1 - \exp(-N\sigma(\lambda)\, l)\, d\lambda \qquad (2.25)$$

where I_o is the spectral irradiance of the incident light,

$\sigma(\lambda)$ is the absorption cross section, and

[1 - exp(x)] is used for the fraction absorption

in a gas-filled collector.

Assuming isotropic irradiance along the optical center of the cylindrically symetric system limits the intensity such that $I = I(\lambda,\varphi, z)$. The absorbed flashlamp power is then

$$P = \int_{z=0}^{z=l} \int_{\varphi=0}^{2\pi} I(\varphi,z)\,(1-r_l)\, d/2\, d\varphi\, dz$$

or

$$P = \int_{z=0}^{z=l} \int_{\varphi=0}^{2\pi} [\int_{250}^{290} I_0(\lambda,\varphi,z)\{1- \exp(-N\sigma(\lambda)\, \lambda d\lambda)\}](1-r_l)\, d/2\, d\varphi\, dz \qquad (2.26)$$

where r_l is the reflective loss of the pump beam at the surface of the laser tube,

l is the pumping length, and

d is the diameter of the laser tube.

The absorption cross section is defined from (1.7) as

$$\sigma(\lambda) = (N_1 - N_2) B_{12} h\nu_{21} \; n. \qquad (2.27)$$

An absorption spectrum for each chemical (C_3F_7I and $C_6F_{13}I$) in this test is shown in figure 8. The spectral match is very close with absorption peaks of 272 and 275 nm for n-C_3F_7I and n-$C_6F_{13}I$, respectively. Bandwidths are 42 and 43 nm (FWHM). This small match of the solar spectrum of perfluoroalkyl iodides, makes the output power directly dependent upon the pump intensity. Figure 9 shows this limited match of the solar and flashlamp spectrum.

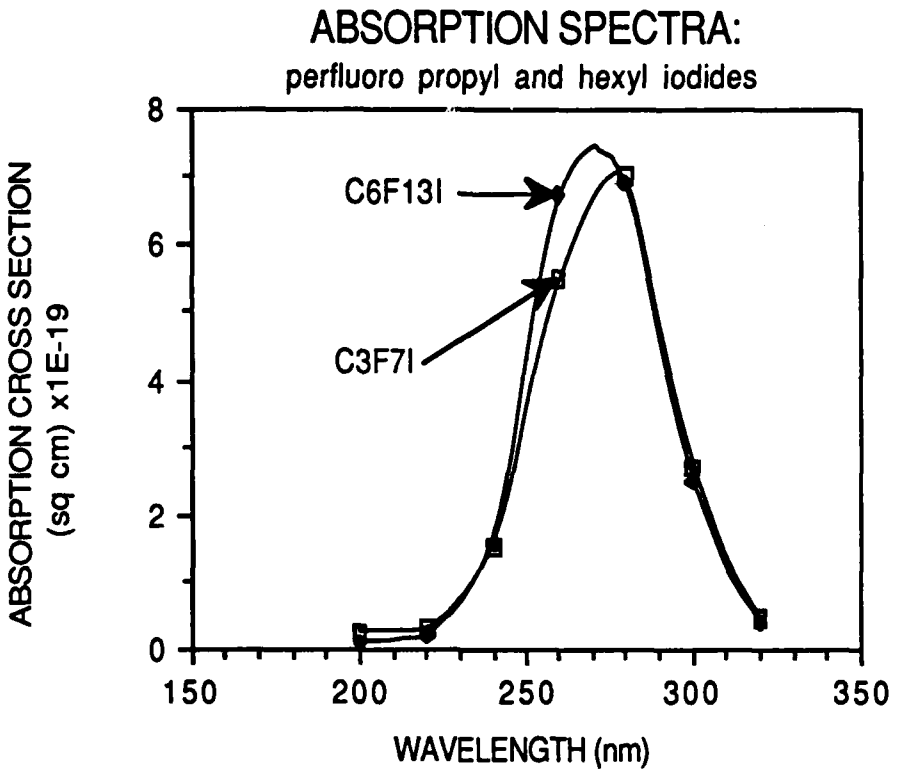

Figure 8. Absorption spectra of the chemicals. The absorption peaks are found between 273 and 277 nm. Absorption is in the UV range from 250 to 300 nm. The absorption widths are 44 and 43 nm respectively.

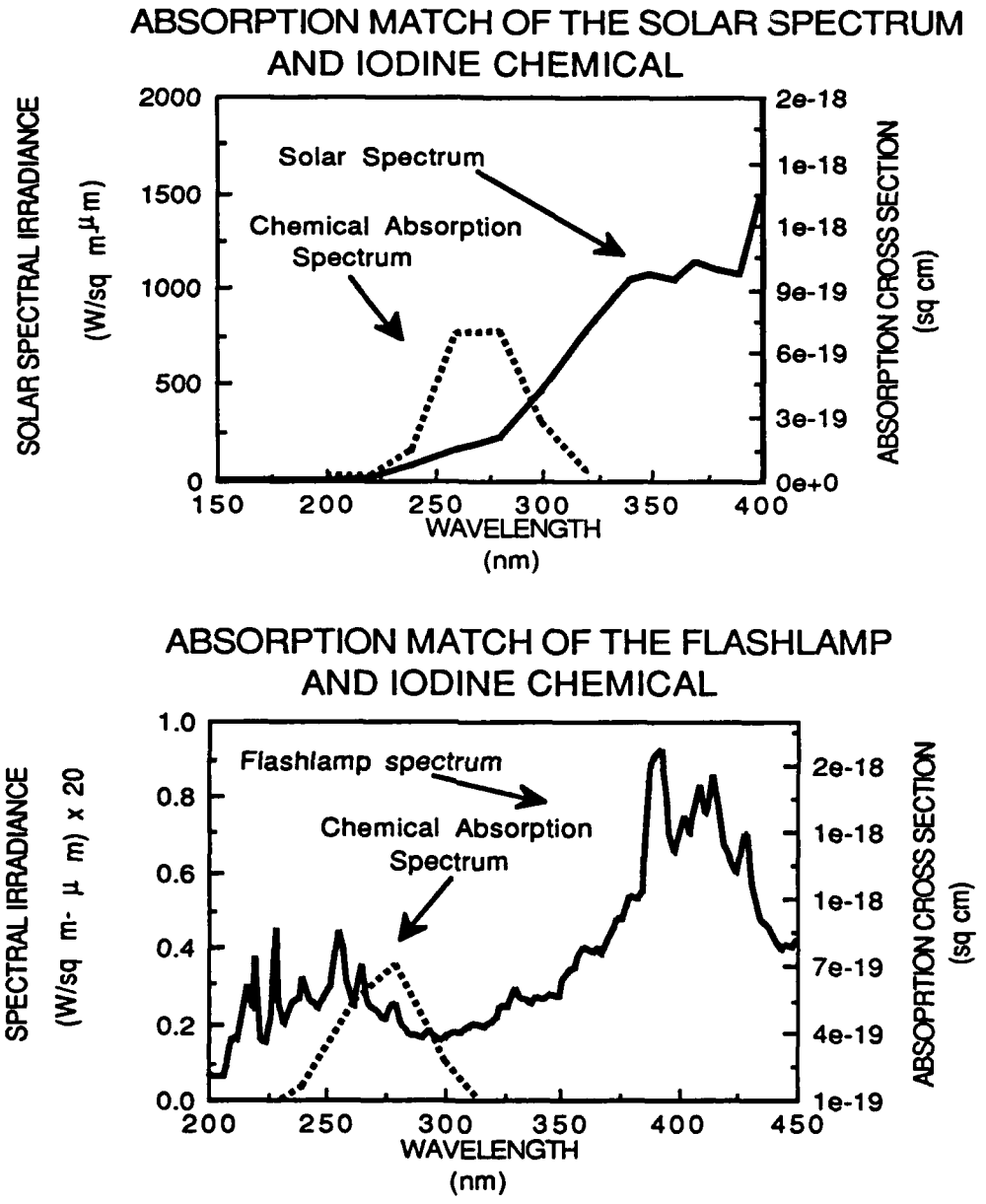

Figure 9. The solar spectrum at Air Mass Zero (AMO) and the spectral match of the flashlamp and the chemical.

Chapter 3

Experimental Set-up and Method

The evaluation of $C_6F_{13}I$ as a suitable lasant is made by the direct comparison of this chemical to C_3F_7I, a well known and throughly tested lasant. In this chapter the investigative methods used in this study are discussed.

A. The Laser System

The iodine laser system was constructed on an Oriel optical table with air bladders used to level the work surface. A 2 m long continuous optical bench was the mounting platform for the system's components. Figure 10 shows a block diagram of the laser system. This system consisted of a 152.5 mm (arc length 101.6 mm) xenon flashlamp coupled to a 6 mm (ID) quartz laser tube by an ellipitical reflector that used aluminum as the reflecting surface. Pumping length was 152.5 mm. The laser tube was 24 cm long. Brewster angle window mounts made of brass capped the ends of the laser tube and provided connection ports to the vacuum/gas delivery system. The laser cavity length was 0.466 m with a 96 percent output and a 99 percent (high IR reflectivity) rear laser mirror .

A red helium-neon laser was fixed to maintain alignment throughout laser testing. Monitoring components included an EG&G

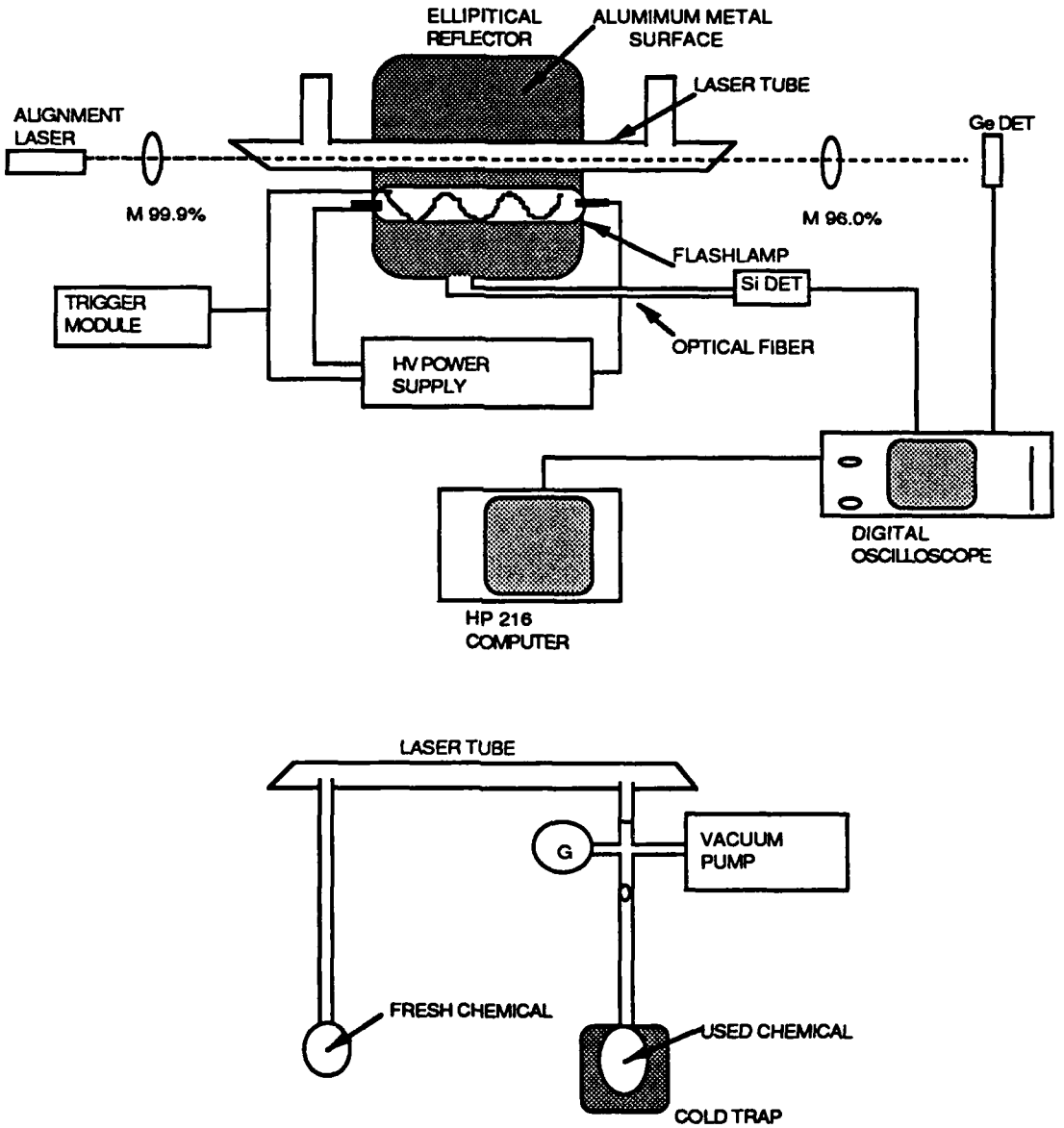

Figure 10. The experimental set-up for the iodine laser system.

silicon photodiode, J-16 germanium detector and a Molectron power-meter. The vacuum system was connected to the laser tube by 0.25 inch stainless steel lines. Polished steel Cajon ® fittings were used throughout the system to provide quick connection. The use of Tygon® tubing was minimized to avoid iodide contatination. A Sergeant-Welch rotary vacuum pump was used to create vacuum conditions below the base pressure 10^{-4} torr.

Figure 11 shows the electrical system used to supply power to the flashlamp. The electrical energy delivered to the flashlamp

$$E_E = 1/2\, CV^2,$$

where C is the capacitance, and V is the charging voltage, ranged from 58 to 138 J. The flashlamp pulse ranged from 900 to 2000μs. Figure 12 indicates a typical flashlamp pulse.

Two chemical flask were mounted below the laser system. One was used as a supply reservoir and the other for collection of the used chemical. Gas filling of the laser tube from the supply reservoir was by vacuum evaporation. Used chemical was collected by freezing in the collection flask which is cooled with liquid nitrogen.

Data acquisition and storage was made by an Nicolet ® (model 201-A) digital oscilloscope interfaced with a Hewlett Packard Model 216 computer. This system provided data storage on both 3.5 and 5.25 inch disks. With the computer data analysis it was possible to obtain screen displayed information as well as printed outputs.

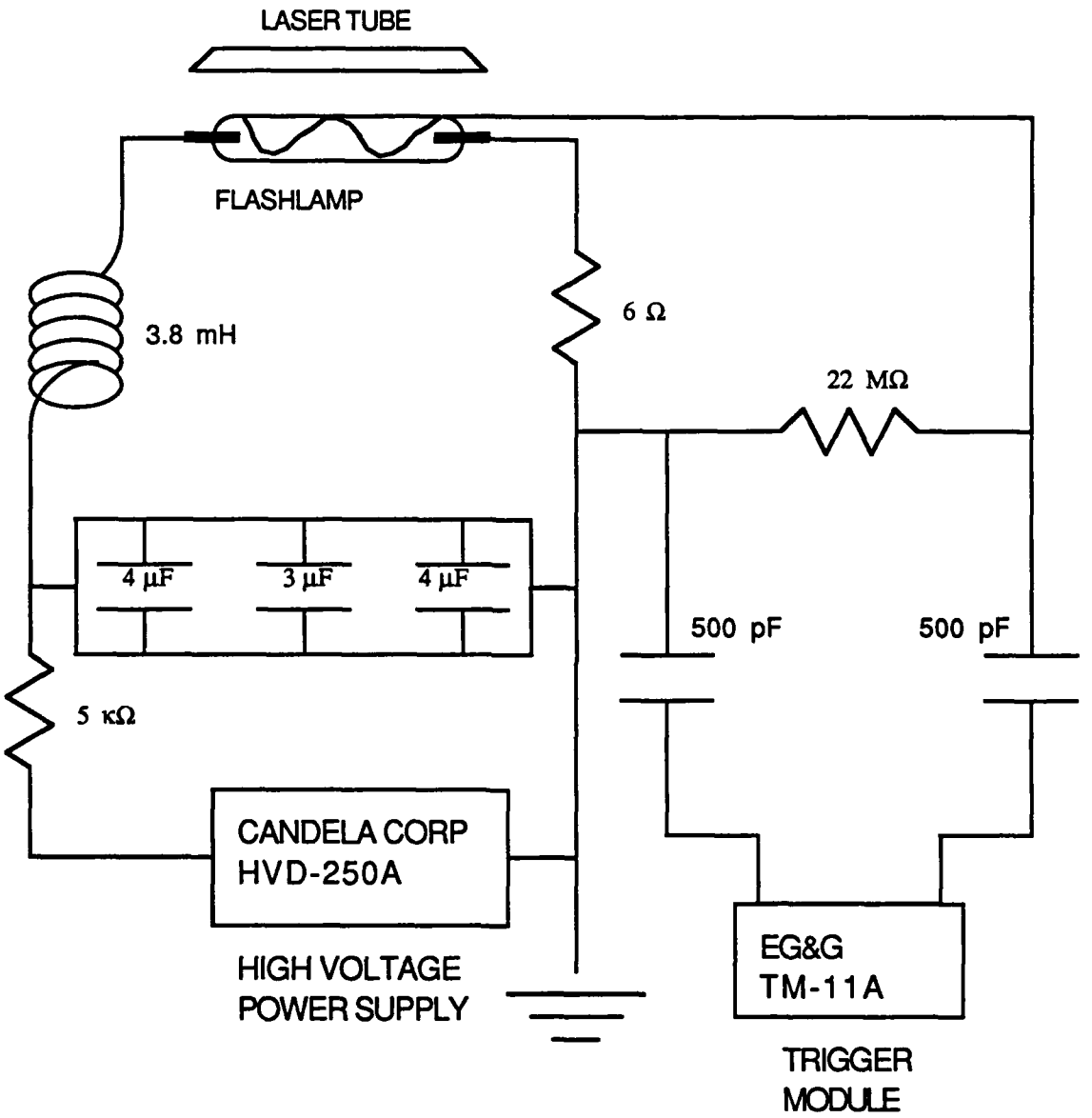

Figure 11. The electrical pump circuit for the iodine laser system.

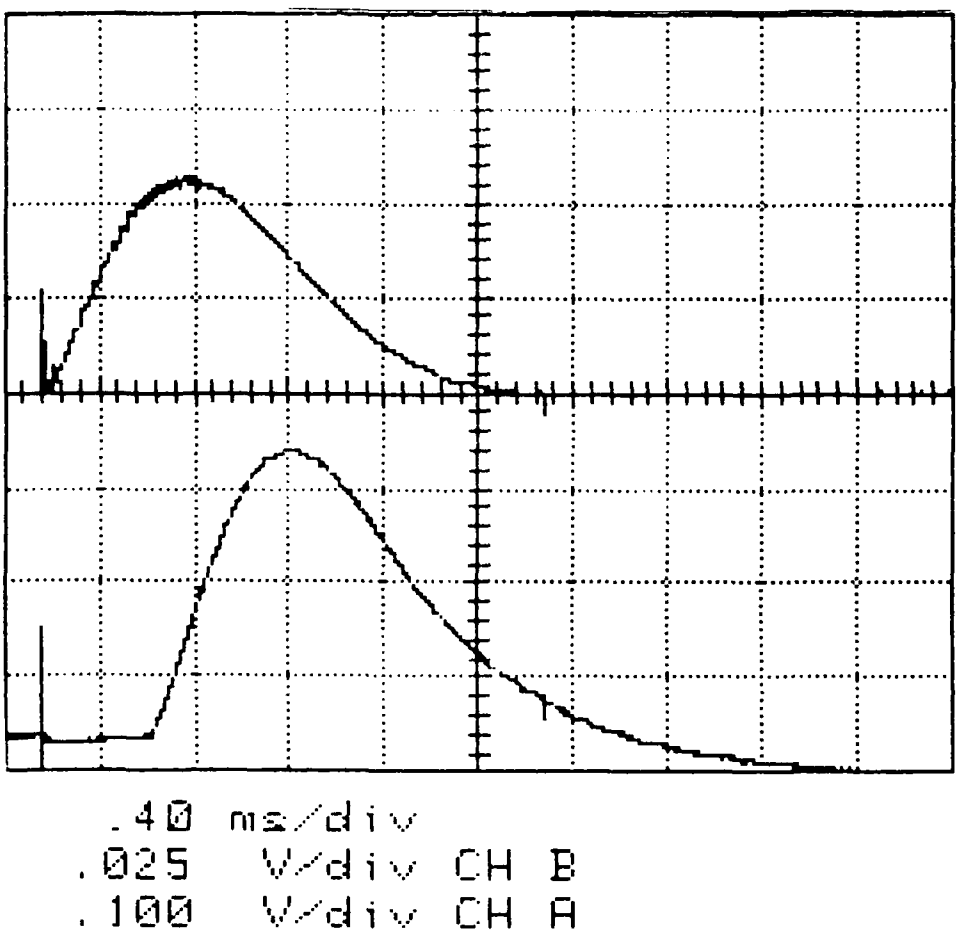

Figure 12. The flashlamp signal (upper trace) read from a digital Nicolet ® oscilloscope. A laser signal is shown on the lower trace.

B. Research Method

1. Laser Output Measurements:

Initially, laser output signals were obtained with used, but distilled C_3F_7I which had a low threshold[16] and therefore, obtaining the first laser signal was easier. Next, careful adjustment of the mirror alignment was made to better tune the system. Initially, the system was at a high Q with the rear and output reflectivities of 99 and 98 percent respectively. To determine the optimum output mirror reflectivity, the laser output and the time to reach threshold against output mirror transmission were measured. The results are shown in figure 13. For transmissions beyond 4 percent the time to threshold becames too high (.500μs), to compare with the time to threshold for $C_6F_{13}I$ which is anticipated to be much higher. In addition, the laser output was lost at transmission above 30 percent. Therefore, it is decided to use 4-percent transmission mirror for the comparison test. Testing, of fresh chemical then began using C_3F_7I. The above process was the preparatory phase of this research. The test that follow were run for C_3F_7I and then $C_6F_{13}I$:

1. Electrical pump energy dependence (pressure constant),
2. Pressure dependence (electrical pump energy constant), and
3. Lasing through repeated runs (Both pressure and electrical pump energy constant).

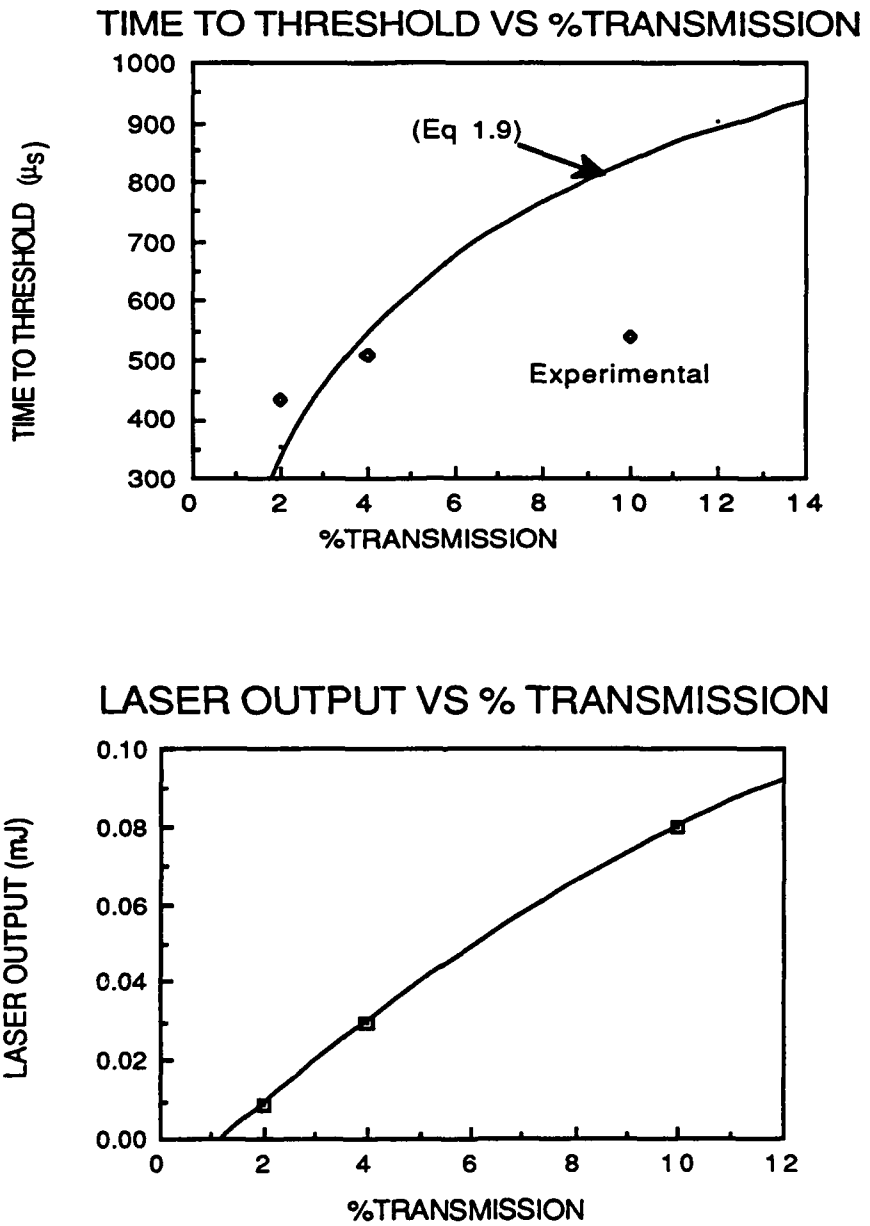

Figure 13. Determination of the time to threshold and laser output for the output mirror transmission. The time to threshold is related to the gain K_{th} in equation (1.9).

After completion of tests with fresh chemicals each test was repeated with used chemical by replacing it in an empty flask. The used chemical that was frozen was heated and flown in a reverse direction through the laser tube and collected in the supply flask. The system was then allowed to pump down two days between test. The results of these test are discussed in the next chapter.

2. Additional Measurements:

a. The absorption spectra for both C_3F_7I and $C_6F_{13}I$ vapor were measured using a Varian® spectrophotometer. This system also used vacuum evaporation to fill a quartz curvette to a specified pressure. The absorption unit read at the peak of the spectrum enabling the absorption cross-section to be calculated from the expression

$$\sigma = -(\ln T) / Nl$$

where T is transmission and equals to $1/10^{AU}$ (AU-Absorption Unit),

N is the number of atoms and equals $(9.65 \times 10^{18}) \times$ (pressure/temp), and

l is the length of curvette.

The absorption range for these measurements were 200 to 345nm. The same techniques were used for liquid samples to determine the relative amount of molecular iodine (I_2) in the sample.

b. The absolute intensity of the flashlamp light in the ultraviolet region to the laser tube was measured using an EG&G Optical Multichannel Analyzer (model 1450A) combined with a Jarrel Ashe

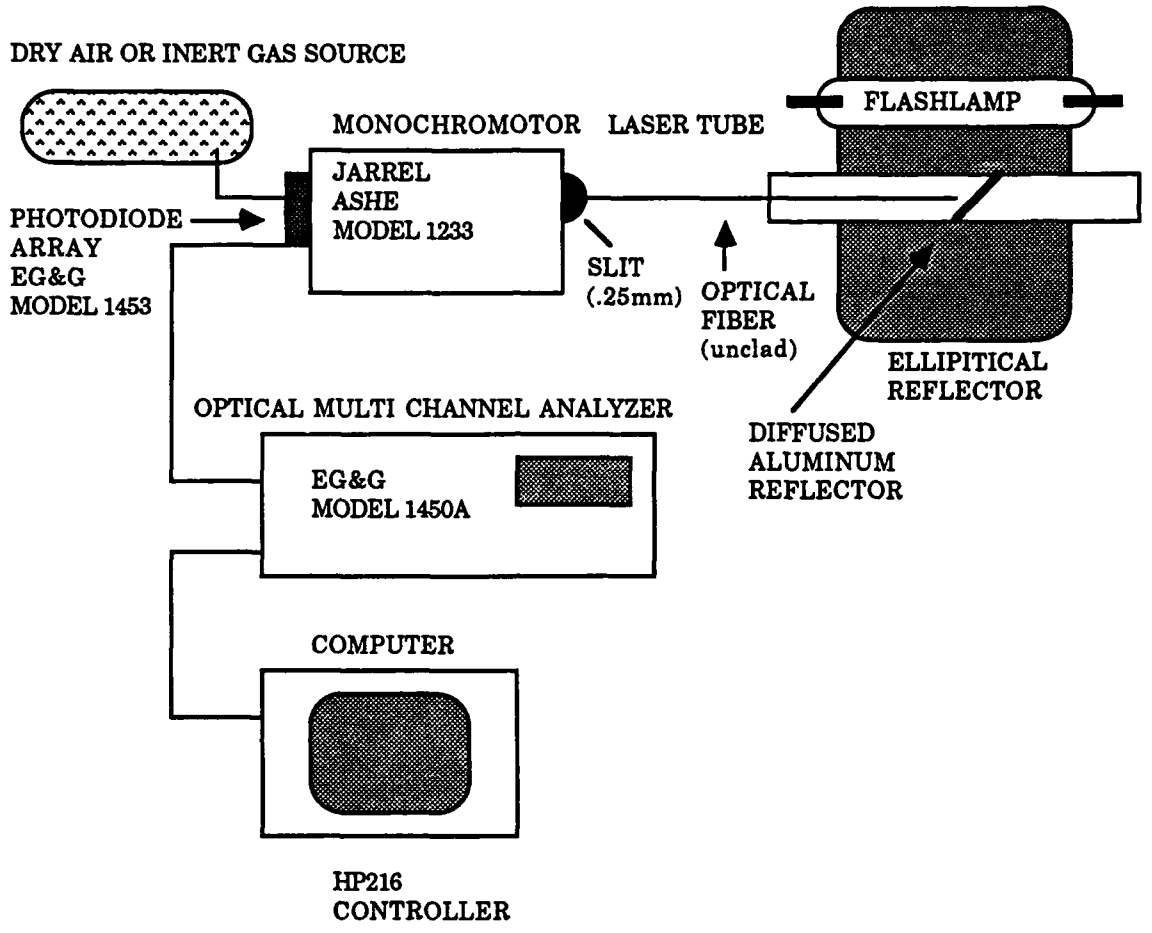

Figure14. Equipment and configuration for the measurement of absolute intensity. A Oriel ® cadmium source was used for initial wavelength calibration. The intensity calibration used an Oriel ® deterium source focused through the laser tube onto a diffused aluminum reflector from a distance of 50 cm.

monochromotor (model 1453). Figure 14 shows the measurement set-up. The absolute irradiance spectrum was determined through direct comparison of the measured flashlamp spectrum (OMA counts) to the irradiance spectrum of a standard UV source (Oriel deterium lamp model 8136). Calculation of the peak intensity in the UV region was by

$$I_p = \{[I_f\ (OMA)/I_c(OMA)] \times I_D\} \times (t_{exp}/t_f)$$

where I_f is the flashlamp irradiance in arbitary units

measured with the OMA,

I_c is the irradiance of the standard source

in arbitary units measured with the OMA,

I_D is the absolute irradiance of the standard source in

power/unit area-wavelength,

t_{exp} is the exposure time for the monochromotor shutter, and

t_f is the pulse duration of the flashlamp.

c. A general measurement of the peak flashlamp energy across the entire spectrum was done using a Molectron Pyroelectric joulemeter (model J-3). The light emitted from the midpoint of the flashlamp (assumning symmetric flashlamp energy at this point) was passed through a UV-superguide fiber and shown onto the detector. A distance of 4.33 cm was placed between the detector and fiber end to simulate the distance between the flashlamp and laser tube. With this system , the approximate energy from the flashlamp radiated upon the pumped area of the laser tube was

$$E_f \approx [(E_d/A_d) \times A_t] \times f_L$$

where E_d is the averge energy measured by the detector,

A_d is the area of the detector ($A_d = 0.02$ cm^2),

A_t is the pumped area of the laser tube ($A_t = 28.73$ cm^2), and

f_L is the correction factor for the loss through the optical fiber.

Chapter 4

Results and Discussion

The direct comparison of C_3F_7I and $C_6F_{13}I$ involved measurements of the absorption coefficients, laser output and production of molecular iodine. Consistency was maintained by performing each test with care holding the un-tested parameters held constant.

A. Absorption Cross-Section

The absorption spectra for C_3F_7I and $C_6F_{13}I$ are shown in figure 14. A determination of the absorption cross-section and related values was taken directly from the absorption spectra as given in Table 4. These values were comparable with those found in Table 5 from reference 20 with the exception for the absorption cross-section of perfluorohexane. Reference 17 found σ to be 7.8×10^{-19} cm^2 for C_3F_7I and 9.1×10^{-19} cm^2 for $C_6F_{13}I$. The values determined in this study were somewhat lower than these values. However the cause of this diference was not pursued.

B. Pump Power

The threshold inversion density was previously determined from (1.13) as

$$\Delta N_{th} = 9.28 \times 10^{14} / cm^3$$

Solving for W in (1.22) gave

TABLE 4.

Absorption Cross-Section Determination

	C_3F_7I	$C_6F_{13}I$
Absorption unit at peak	.048	.049
Transmission [T=1/10^{AU}]	.895	.893
No. of Molecules in a Standard Volume [n=9.656x10^{18}P/T]	3.48x10^{17}	3.23x10^{17}
Absorption Cross-Section (cm^2) [σ= -lnT/nl] l=.5 cm	6.8x10^{-19}	7.0x10^{-19}
Peak Absorption Wavelength (± 0.6 nm)	273.9	277.3
Absorption Width (± 1.2 nm) $\Delta\lambda$(FWHM)	44.4	43.1

TABLE 5.

Comparison values from Reference 20

Absorption Cross-Section (cm^2)	6.6x10^{-19}	6.0x10^{-19}
Peak Absorption Wavelength(nm)	273	272
$\Delta\lambda$ (nm)	42	42

TABLE 6.

Mimimum Pump Power

Elec Pump Energy (Joules)	Fresh chemical Time to threshold (μsec)*	Fresh chemical Minimum pump power (Watts)*	Used chemical Time to threshold (μsec)*	Used chemical Minmum pump power (Watts)*
58.1	503/436	2.07/1.98	490/487	2.06/2.05
67.4	469/414	2.01/1.94	476/449	2.00/1.98
88.0	418/339	1.91/1.81	402/372	1.89/1.85
98.4	405/322	1.87/1.78	368/358	1.83/1.82
111.4	366/317	1.66/1.62	348/330	1.65/1.63
124.0	350/312	1.57/1.54	324/317	1.55/1.54
138.0	346/296	1.50/1.46	321/307	1.47/1.46

* The values for C_3F_7I and $C_6F_{13}I$ are listed together separated by a slashes.

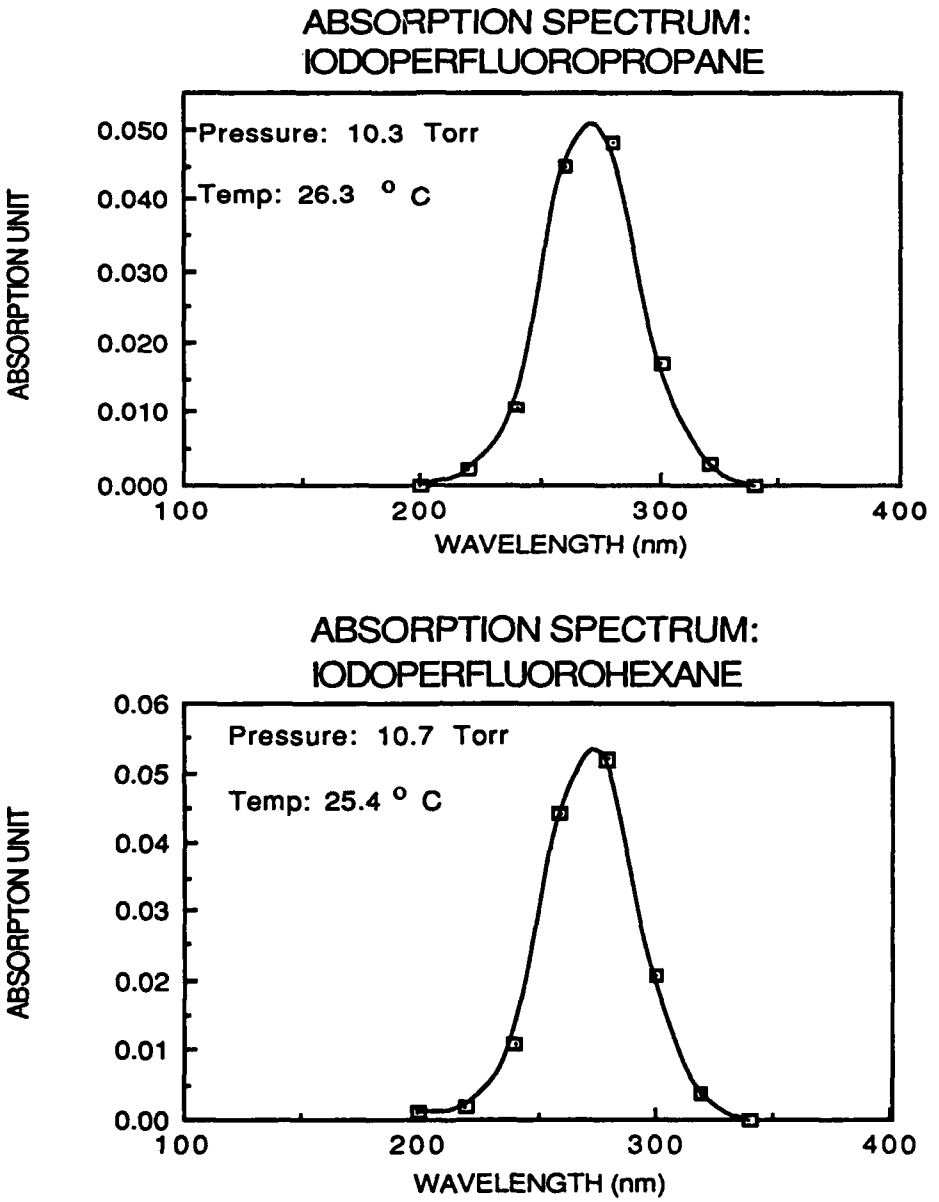

Figure 15. Absorption spectra obtained from the Varian ® spectrophotometer for C_3F_7I and $C_6F_{13}I$. Three measurements were taken for each chemical and the average of the acceptable values used to calculated the absorption cross section of each chemical.

$$W \approx \Delta N h\nu V / t_{th} \qquad (4.1)$$

Using the time to threshold as the pumping duration the value for the minimum pump power was found as in Table 6. Perfluorohexane requires more power to reach lasing even for fresh chemical. After several trials the optimum conditions for laser output was obtained for $C_6F_{13}I$. It turn out that the minimum pump power for $C_6F_{13}I$ was even less than that for C_3F_7I, and the output energy was then also greater.

C. Absolute Intensity

The absolute intensity of the pumping light in the ultraviolet region was measured at electrical energy from 58 joules up to 138 joules. Table 7 shows the results of this measurement. The irradiance values are at λ=239 nm and the energy values are the total incident energy in 200 to 300 nm band into the laser tube. Figure 17 show that the electrical energy conversion to optical energy had an averaged efficiency of 2.6 percent.

D. Laser Output

Laser output was measured for fresh and used chemicals while varying the gas pressure and electrical energy. Figures 18 to 21 show the results of these tests. Throughout testing $C_6F_{13}I$ produced laser outputs that exceeded perfluoropropane for the same pressure or the same pump power. The highest output for $C_6F_{13}I$ was 1.5 times higher than that of perfluoropropane at the

pressure of 13 torr for 67 J electrical input energy (figure 20). This result agrees with reference 4 that predicted $C_6F_{13}I$ to be a more efficient working media among heavier fluorinated alkyl iodides. It differs from reference 3, which reported the output of C_3F_7I and $C_6F_{13}I$ to be almost equal under CW operation.

E. Single Charge Performance

The degradation of the lasant resulting from repeated laser excitation was measured by the decrease of laser output for single gas charge until there was no laser signal obtained. A 1 minute time interval was placed between each firing of the flashlamp. Figures 22 and 23 show the results of this test. Although $C_6F_{13}I$ yielded a higher output, lasing by this chemical ended after only 13 runs. While with C_3F_7I, lasing continued up to 25 runs. This fact indicated that $C_6F_{13}I$ reconstitution is relatively slow compared with C_3F_7I.

F. Molecular Iodine Production

Molecular iodine (I_2) is an undesirable product in an iodine laser system. It strongly quenches lasing by reducing the number of excited iodine atoms. Table 8 shows the spectral absorption values and number density calculation for chemical. The number of I_2 molecules were determined from the equation

$$N = -\ln(\Delta T) / \sigma_3 l \qquad (4.2)$$

where ΔT is the change in transmission for fresh and used chemicals, and σ_3 is

the change in the absorption by I_2 in the range 450-550nm, for fresh and used chemical. The visible evidence of this fact is also observed in figure 24, which shows greater absorption for used C_3F_7I than for used $C_6F_{13}I$. This higher absorption is due to the increase in molecular iodine molecules. Perfluoropropane was found to produce almost 40 times more molecular iodine than $C_6F_{13}I$ when used in an iodine laser system. In order for this to occur, photodissociation I_2 may be captured by the radical producing more parents molecule. This assumption may be viable based on the number of runs from a single filling test. With photodissociated I_2 competing with I* to form more I_2 after transition to the $5^2P_{3/2}$, and laser transition, recombination to the parent molecule is slower. Slow recombination would then impede pumping of iodine atoms into an excited level affectively quenching the laser. When a time longer than one minute was used between each run the laser output returned.

G. Threshold - Reflectivity Dependence

The dependence of threshold conditions on reflectivity is drawn from basic laser theory. Equation (1.9) defined threshold conditions as

$$G=r_1r_2\exp[2(K_{th}-\gamma)L)=1.$$

Assumning losses to be neglectible, and substitution of equation (1.13) provides

$$G= r_1r_2\exp(2_{\sigma s}\Delta N_{th}L) \qquad (4.3)$$

where σ_s the stimulated emission cross section (=5.0x10^{-18} cm^2) is

$$\sigma_s= 1/(8\pi\nu_o^2\,\tau_{2\,1}\Delta\nu\, n^2/c^2).$$

Solving (4.3) for ΔN_{th} shows the dependence of the threshold inversion density on reflectivity

$$\Delta N_{th} = -\ln(r_1 r_2)/2\,\sigma_s L.$$

The threshold inversion density for output mirror reflectivities of 98, 96.and 90 percent (rear mirror fixed at 99 percent) are shown in table 9. These values indicate that the threshold inversion density is inversely proportional to the reflectivity of the output mirror. Direct comparison with figure 13 show that reflectivity is inversely proportional to the time to reach threshold. Therefore, the threshold inversion density is directly proportional to the time to reach threshold.

TABLE 7.

Absolute Intensity of the Flashlamp

Charging Voltage(kV)	Electrical Energy(J)	Irradiance (W/cm^2nm)	Power (Watts)	Energy (mJ)
3.25	58.1	6.09×10^{-3}	7.30	1.79
3.50	67.4	6.65×10^{-3}	8.02	1.95
4.00	88.0	7.90×10^{-3}	9.60	2.33
4.25	111.4	9.43×10^{-3}	11.37	2.76
4.50	124.0	1.02×10^{-2}	12.26	2.98
5.00	138.0	1.07×10^{-2}	12.89	3.13

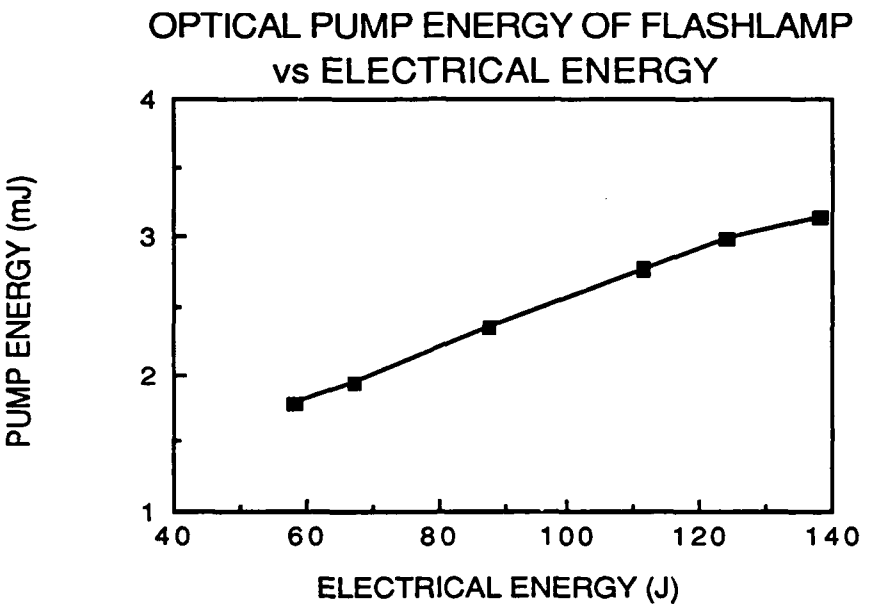

Figure 16. Optical pumping energy compared to input electrical energy.

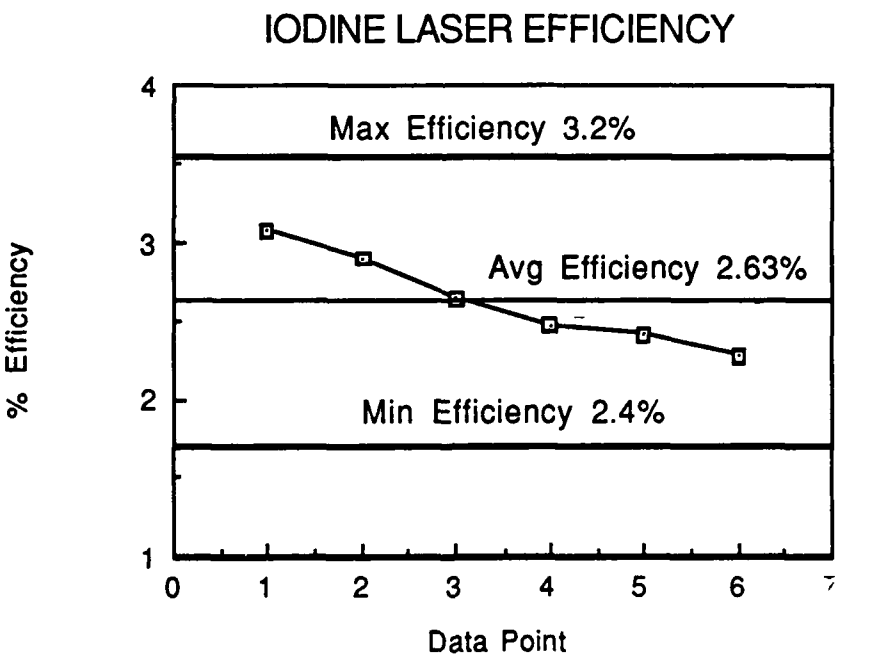

Figure 17. The optical efficiency of the iodine laser system.

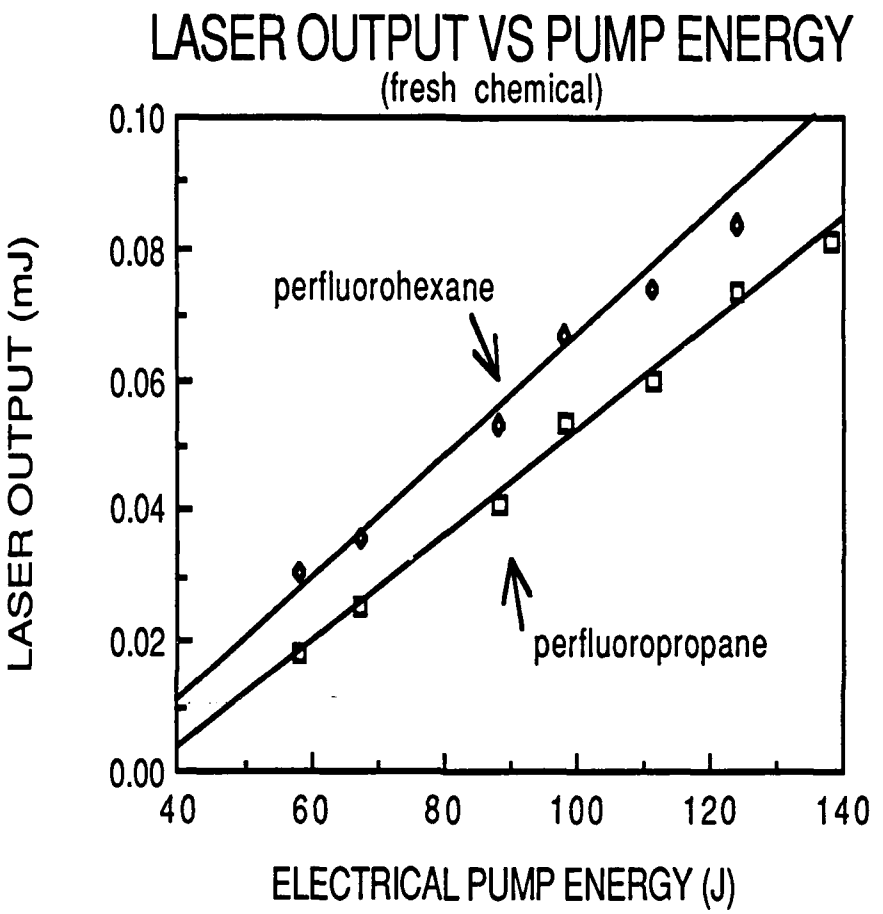

Figure 18. Laser output compared to the input electrical pump energy for fresh $C_6F_{13}I$ and fresh C_3F_7I at pressure 10.3 Torr.

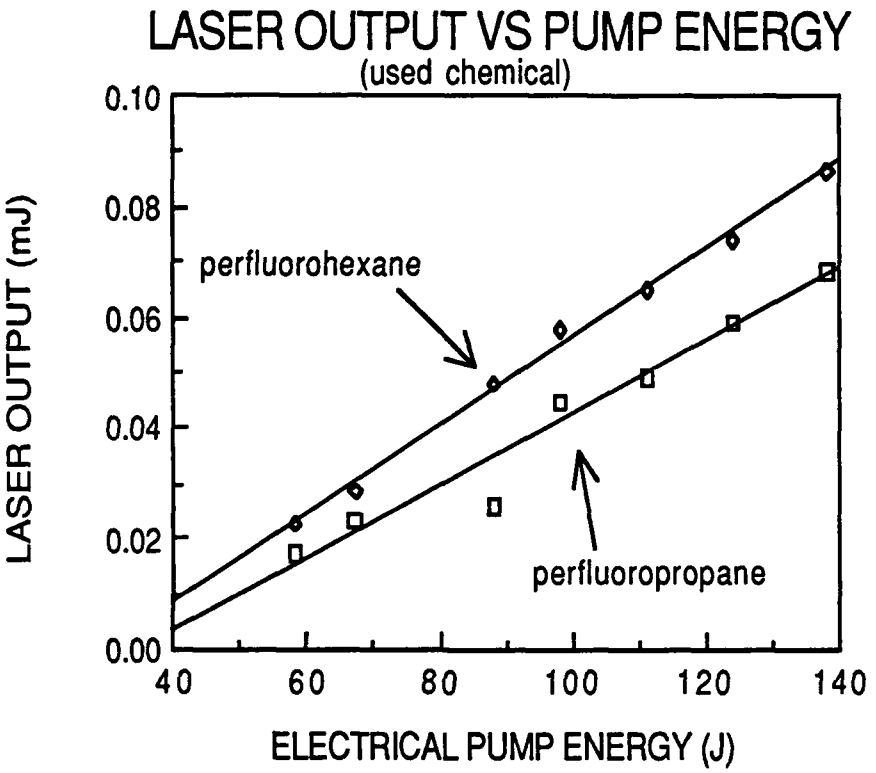

Figure 19. Laser output compared to electrical pump energy for used $C_6F_{13}I$ and used C_3F_7I at pressure 10.3 Torr.

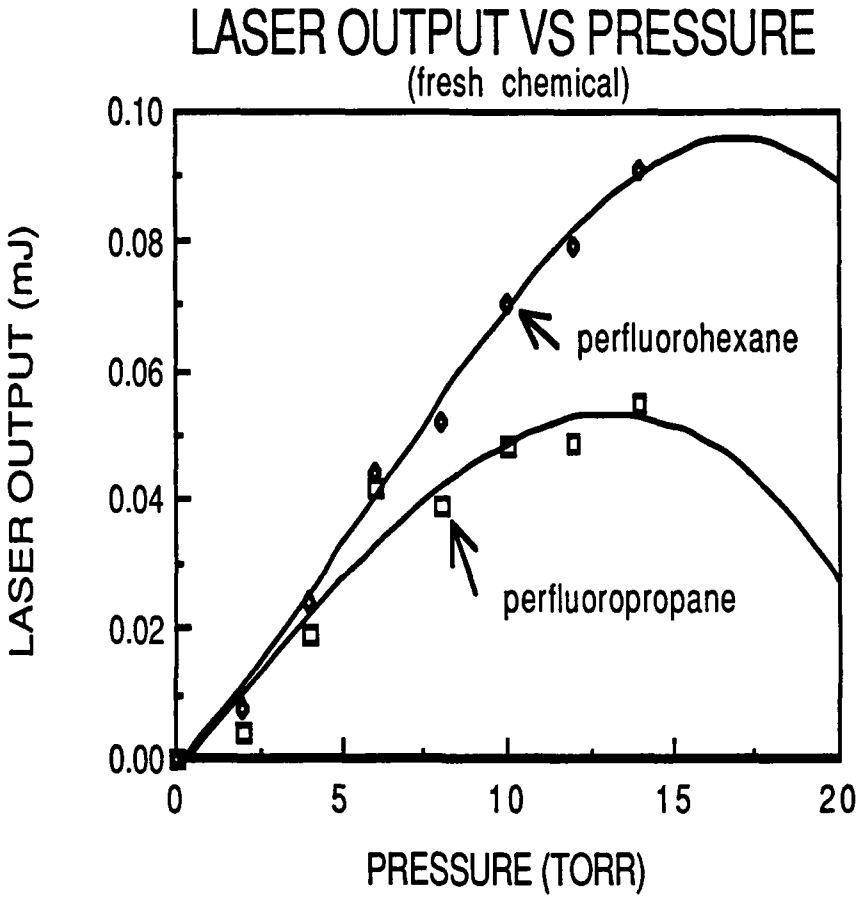

Figure 20. Laser output compared to gas pressure for fresh $C_6F_{13}I$ and fresh C_3F_7I. The smooth curve represents a polynominal fit to the data. The electrical energy used was 67 J.

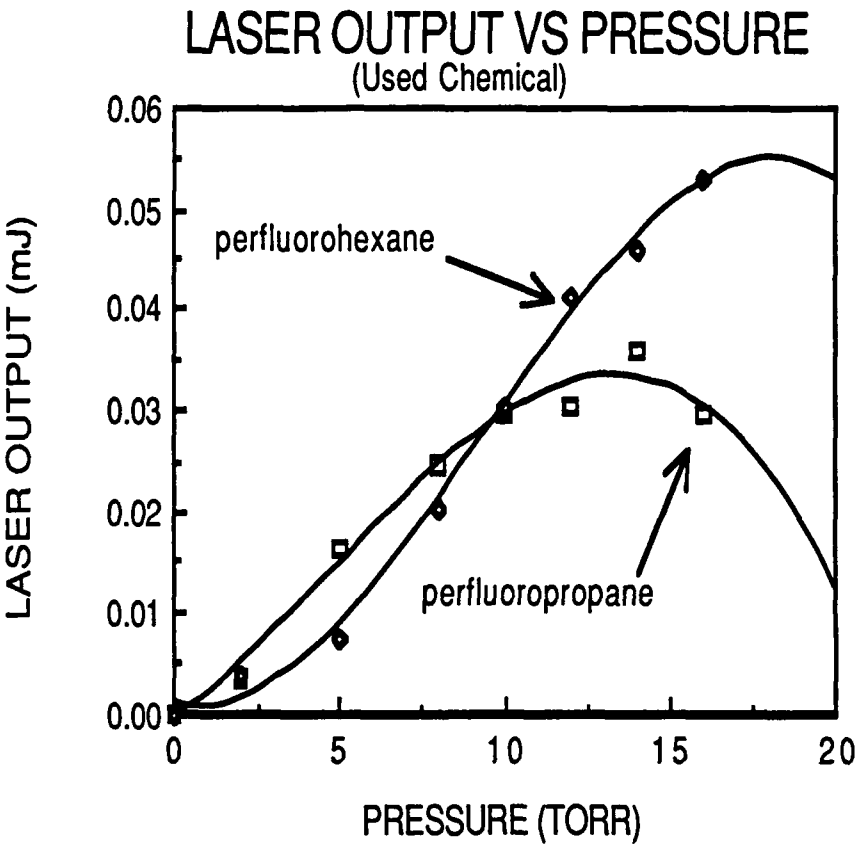

Figure 21. Laser output compared to gas pressure for used $C_6F_{13}I$ and used C_3F_7I. Again, the smooth curve represents a polynomial fit to the data. Perfluorohexane initially had laser output below C_3F_7I, but improved with use and increased gas pressure. The electrical energy used was 67J.

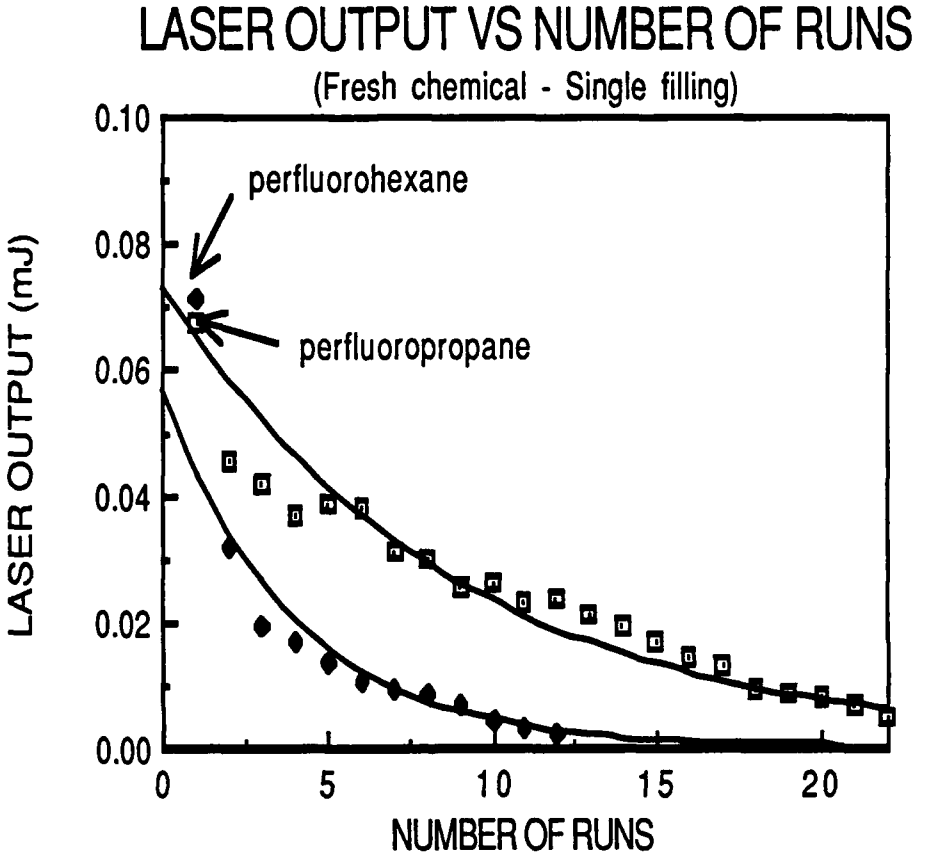

Figure 22. Laser output compared to repeated firing of the laser system with a single filling of gas using fresh chemical at 11 torr. Perfluorohexane had only 13 runs before no laser signal was read as opposed to C_3F_7I which lased up to 24 runs. The electrical energy used was 67J.

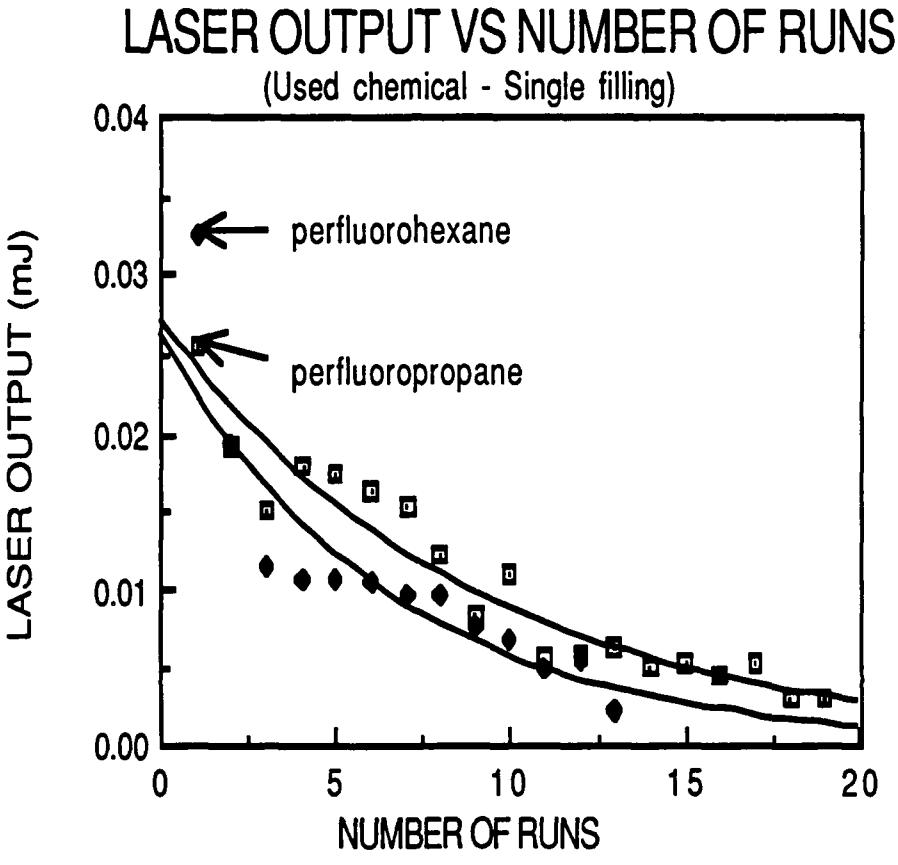

Figure 23. Laser output compared to repeated firing of the laser system with a single filling of gas with used chemical at pressure of 11 torr. Perfluorohexane again lased through 13 runs while lasing ended for C_3F_7I after 20 runs. The electrical energy used was 67J.

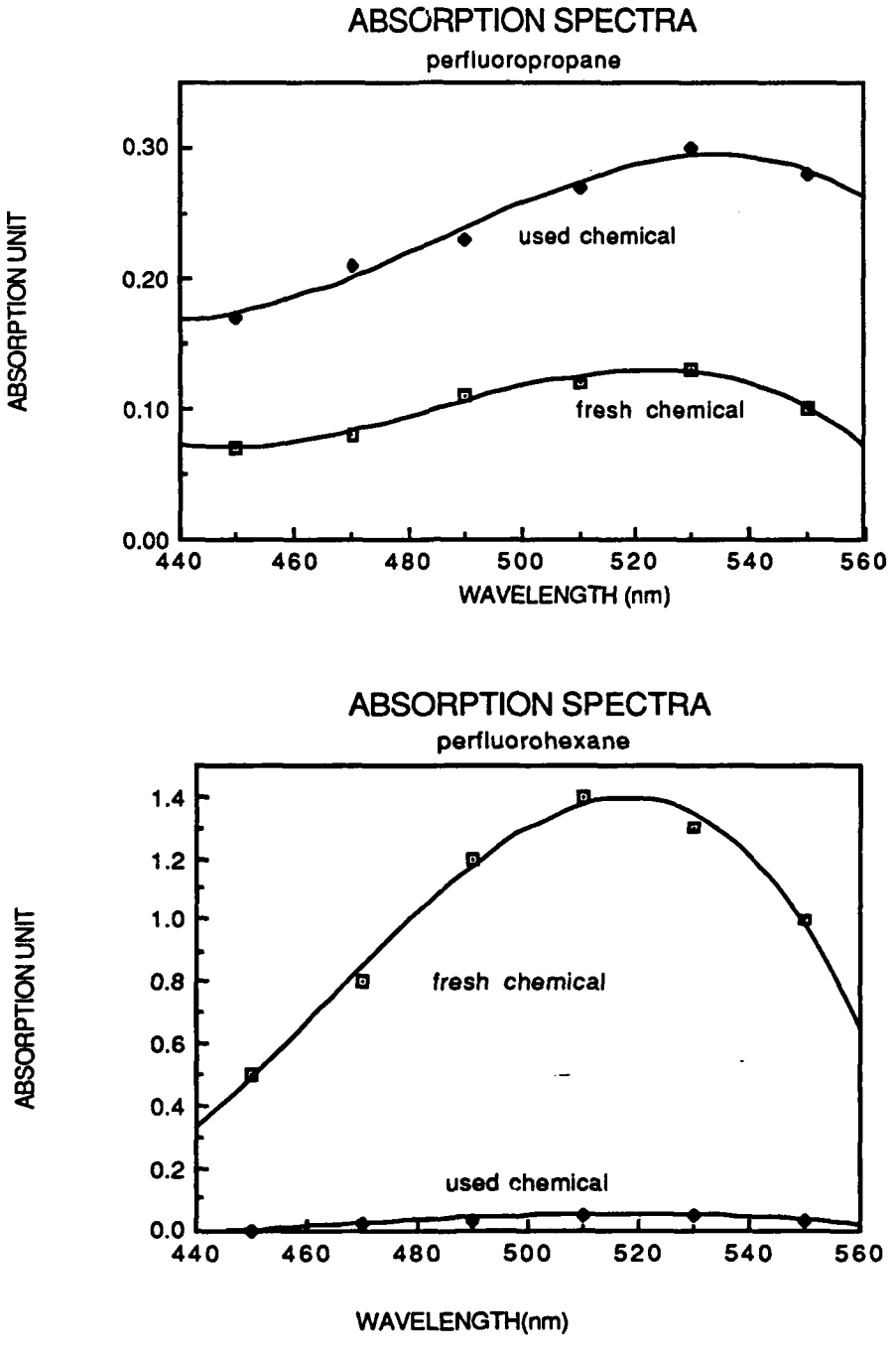

Figure 24. Absorption spectra for fresh and used C_3F_7I and $C_6F_{13}I$ in the visible region 450 to 550 nm. The peak absorption was used to determine I_2 production.

TABLE 8.

Molecular Iodine Production Determination

Chemical*	Fresh Chemical*	Used
Absorption unit a peak	.127/1.405	.296/.052
Transmission[T=1/10^{AU}]	.74/.03	.50/.88
Absorption Cross Sections (cm^2)	1.25×10^{-22}/ 1.39×10^{-19}	2.93×10^{-20}/ 5.15×10^{-21}

*Values are listed as $C_3F_7I/C_6F_{13}I$

	C_3F_7I	$C_6F_{13}I$
Difference in Absorption Cross Sections for fresh and used chemical (cm^2)	2.9×10^{-20}	1.34×10^{-19}
No. I_2 molecules produced	9.76×10^{19}	2.46×10^{18}

TABLE 9.

Reflectivity - Threshold Dependence

Percent Reflectivity (r_1)	(r_2)	Threshold Inversion Density (cm^3)	Time to Threshold (μs)
99	98	2.4×10^{14}	430
99	96	5.0×10^{14}	515
99	90	9.2×10^{14}	540

r_1 - rear mirror, r_2 - output mirror

Chapter 5

Conclusion

This study has shown that $C_6F_{13}I$ produces higher outputs and less molecular iodine than C_3F_7I when used in a long pulse iodine laser system. In addition that subtle differences exist in the iodine laser kinetic for $C_6F_{13}I$ that affect its output energy, molecular iodine production and recombination back into the parent molecule.

The measured absorption cross sections of the chemicals differs by only 3 percent. This small difference means little variance in the amount of energy absorbed. Additionally, thechemical have little difference in absorption peaks (272 to 275 nm) and absorption bandwidths (42 and 44 nm). Consequently, the pump power absorbed does not account for the difference in laser outputs of the two chemicals.

Nevertheless, as shown in table 6 $C_6F_{13}I$ was found to be a better lasant based upon its shorter time to reach threshold and lower threshold pump power. The reason for the better laser performance of $C_6F_{13}I$ may be due to the fact that in the lasing process the chemical quality of the $C_6F_{13}I$

improved. The visible evidence of this improvement was a color change from red to clear.

The iodine laser is limited by its absorption band in the ultraviolet. This region has the lowest energy of the solar spectrum. Measurements of the flashlamp light incident on the laser tube show 56 and 100 mJ for 58 and 88 J electrical energy respectively. Absolute intensity in the UV for these pump energies were 1.79 and 2.33 mJ, respectively. On the average, only a few percent of the available energy from the flashlamp was used in pumping the laser.

Perfluorohexane consistently produced higher laser output than C_3F_7I for the same pressure or the same pump energy. For used chemical, $C_6F_{13}I$ initially had output below that of C_3F_7I. However, this condition reversed as the pressure of $C_6F_{13}I$ ncreased.

The factors leading to this higher output may be due to the process which reduces molecular iodine. With more iodine atoms, the reactions such as

$$2I + M \rightarrow I_2 + M$$

where M is a reacting agent (,i.e. O_2 or I_2) and

$$I^* + I_2 \rightarrow I_2 + I$$

should occur with more frequency, producing more molecular iodine. The latter quenches the upper laser level. Examination of Table 2 shows five reactants which react to produce molecular iodine. But, the used $C_6F_{13}I$ contains a reduced the amount of I_2 present as shown by spectrophotometer measurements. Iodoperfluorohexane provides higher output energy and reduces I_2 each time it is used.

The pressure for the highest output from $C_6F_{13}I$ was the maximum vapor pressure at room temperature. This is advantageous for a static filling system, but the low vapor pressure may make it difficult to maintain a fast flow for continuous wave operation. The higher density and associated higher specific heat will allow operation under higher pump power than that possible with other perfluoroalkly iodides therefore, reducing the radiator size for a space system. Exploiting the self-improving quality of this chemical would reduce the need for frequent distillation, again reducing the design load for an orbiting power generation station. Therefore, $C_6F_{13}I$ is found to be a suitable alternative to C_3F_7I for pulsed high energy iodine laser systems. It has advantages over C_3F_7I in both

laser performance and chemical quality. The exploitation of its self-improvement quality means a reduction in the needed distillation of a closed iodine laser system. Overall perfluorohexane meets the requirements for applications in iodine laser systems in laboratories or in space laser power transmission.

REFERENCES

1. B. Elson, Aviation Week & Space Technology, 86 (1984).

2. W. R. Weaver, and J. H. Lee, J. Energy. 7, 6 (1983).

3. B. M. Tabibi, J. H. Lee, and W. R. Weaver, Am. Phy. Soc Bull. 31, 1756 (1986).

4. G. A. Skorbogator, V. G. Seleznev, B. N. Makismov, and O. N. Slesar, Sov. Phys. 20, 1533 (1975).

5. E. Hecht, "Optics", Addison-Wesley Publishing Co. (USA) 1989.

6. G. Brederlov, E. Fill, and K. J. Wittle, "The High-Power Iodine Laser", Springer-Verlag, Berlin Heiderberg, New York, 1983.

7. K. S. Han, and Y. J. Shiu, Semi-Annual Progress Report: NAG-1595 (1979).

8. J. V. Kasper, and G. C. Pimentel, Appl. Phys. Letters 14, 231 (1964).

9. J. W. Wilson, Y. Lee, W. R. Weaver, D. Humes, and J. H. Lee, NASA Technical Paper 2241 (1984).

10. S. V. Kuzentsova, and A. I. Maslov. Sov. J. Quant Electron. 8, 906 (1978),

11. C. C. Davis, R. J. Prikle, R. A. McFarlane, and G. J. Wolga, IEEE J. Quant Electron. QE-12, 6 (1976).

12. F. T. Aldridge, IEEE J. Quant. Electron. QE-11, 215 (1975).

13. T. D. Padrick, and R. E. Palmer, J. Chem. Phys. 62, 3350 (1975).

14. A. L. Golga, and I. I. Klimovskii, Sov. J. Quant Electron. 14, 2 (1984).

15. R. J. De Young, Appl. Optics. 25, 21 (1986).

16. J. H. Lee, M. H. Lee, and W. R. Weaver, "High Power CW Laser Pumped By Solar Simulator", Proceedings of the International Conference on Laser, (1986).

17. M. A. Pollack, Appl. Phys. Letters 8, 36 (1966).

18. E. Gerck, J. Chem. Phys. 79, 311 (1983).

19. A. J. DeMaria, and C. J. Ultee, Appl. Phys. Letters 9, 67 (1966).

20. J. H. Lee, B. M. Tabibi, D. H. Humes, and W. R. Weaver, AIP. Conf. Proc. 172, Advances in Laser Science III, 109 (1988).

21. J. H. Lee, B. M. Tabibi, D. H. Humes, and W. R. Weaver, Opt Comm 74, 380(1989).

22. C. M. Ferrar, Appl. Phys. Letters 12, 11 (1968).

23. S. Glasstone, K. J. Laider, H. Eyring, "The Theory of Rate Processes", McGraw Hill Book Co., Inc. (New York) 1941.

24. C. H. Yoder, F. H. Suydom, F. A. Snavely, "Chemistry", Harcourt

Brace Jovanorich, Inc. (New York), 1980.

25. D. W. Gregg, R. E. Kidder, and C. V. Dobler, Appl. Phys. Letters 13, 297 (1968).

26. J. Wilson, and J. F. B. Hawkes, "Optoelectronics, An Introduction", Prentice Hall International (UK), 1989.

27. E. A. Yukov, Sov. J. Quant. Electron. 3, 177 (1973).

28. R. J. De Young, G. H. Walker, M. D. Williams, G. L. Schuster, and W. J. Conway, NASA Technical Morandum 4002, (1987).

29. P. Gensel, K. Hohla, and K. L. Kompa, Appl. Phys. Letters 18, 48 (1971).

30. J. W. Wilson, S. Raju, and Y. J. Shiu, NASA Technical Paper 2182 (1983).

31. K. S. Han, and Y. J. Shiu, Annual Progress Report: NAG-1595, (1981).

32. V. V. Grigoryants, M. E. Zhabotinski, and V. M. Markeshev, IEEE J. Quant. Electron. QE-8, 196 (1972).

33. J. A. Blake, and G. Burns. J. Chem. Phys. 54, 1480 (1971).

34. N. G. Basov, L. E. Golubev, V. S. Zuev, V. A. Katulin, V. N. Netemin, V. Yu. Nosach, O. Yu. Nosach, and A. L. Petrov, Sov. J.

Quant Electron. 3, 524 (1974).

35. S. V. Kuzetsova, and A. I. Maslov. Sov. J. Quant Electron. 3, 468 (1974).

36. J. W. Wilson, NASA Technical Memorandum: 81894 (1980).